Lithium-mediated nitrogen reduction for ammonia synthesis: reviewing the gap between continuous electrolytic cells and stepwise processes through galvanic LiN2 cells

Vol. 14 • No. 25 • July 5 • 2024
www.advenergymat.de

ADVANCED ENERGY MATERIALS

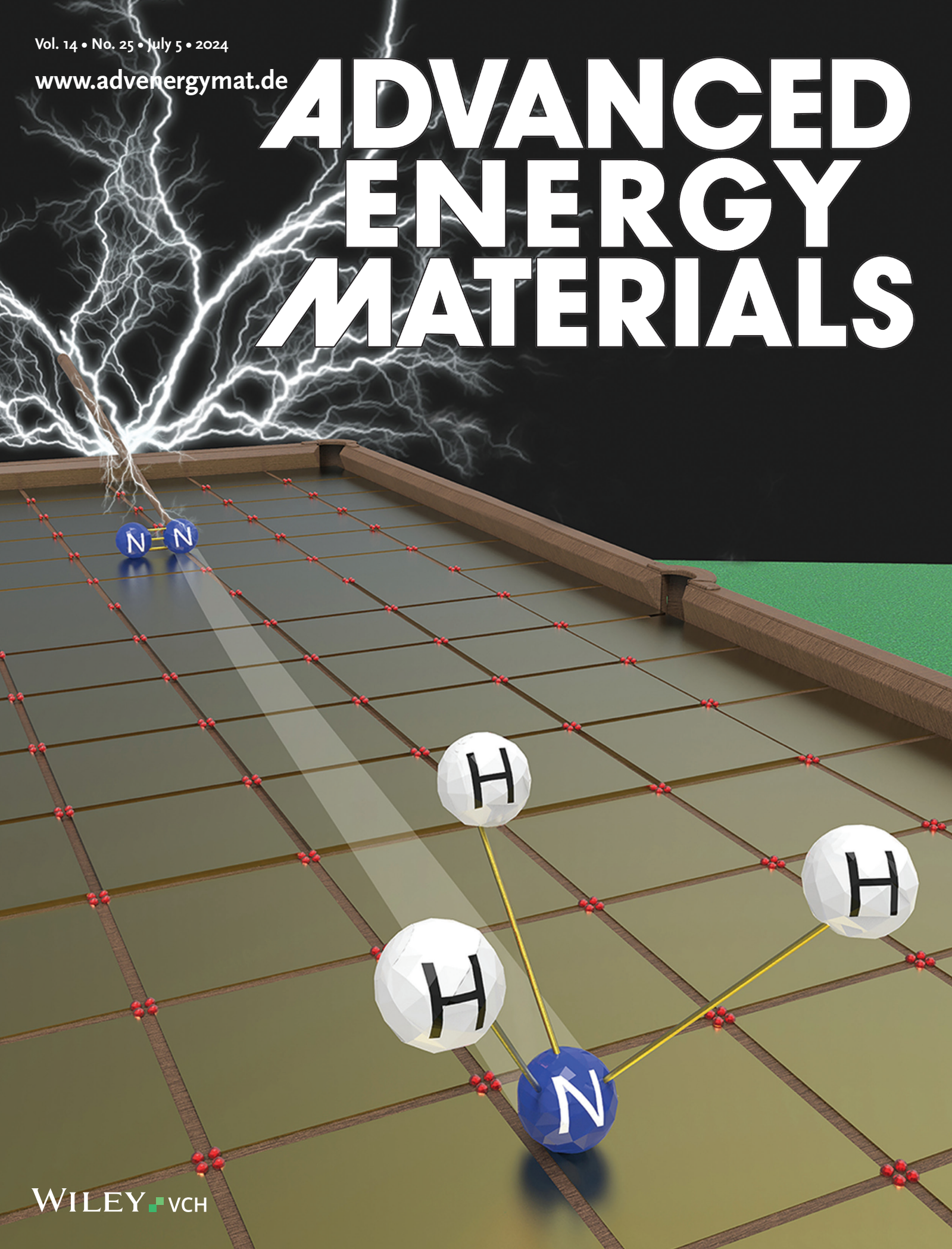

WILEY VCH

ADVANCED ENERGY MATERIALS
www.advenergymat.de

Lithium-Mediated Nitrogen Reduction for Ammonia Synthesis: Reviewing the Gap between Continuous Electrolytic Cells and Stepwise Processes through Galvanic Li—N_2 Cells

*Anna Mangini, Lucia Fagiolari, Annalisa Sacchetti, Alberto Garbujo, Pierdomenico Biasi, and Federico Bella**

Electrochemical N_2 reduction reaction (E-NRR) has recently gained increasing interest within the scientific community, due to the ongoing energy crisis and pursuit of process sustainability. In this scenario, emerging lithium-mediated (Li-m) strategies are obtaining promising Faradaic efficiency (FE) and NH_3 production rate values. In this work, the Li-m scenarios are classified and explained toward a more sustainable process. Continuous processes, with a lithium salt and a proton donor in an electrolytic cell, are analyzed and compared with stepwise pathways. Different parameters are summarized in relation to the system stability, for which the importance of a tailored solid electrolyte interphase (SEI) layer emerged. Among stepwise processes, the thermochemical direct nitridation of lithium is discussed together with the recently developed Galvanic Li—N_2 cell strategy.

1. Introduction

Ammonia, one of the top-3 chemicals produced worldwide, is at the base of fertilizer synthesis and its production will increase further with demographical growth.[1] The availability of a distributed NH_3 production could ensure independence on these essential goods, in particular for developing countries. Moreover, the idea of using liquid NH_3 as a viable green energy carrier has been gaining interest in recent years, since it is more easily transportable and safer than H_2.[2] This molecule is a promising alternative to carbon-based fuels. However, N_2 fixation still represents a huge challenge due to the stable triple bond of the non-polar N_2 molecule, which requires extreme conditions to promote the reduction kinetics.[3]

Operating under severe temperature and pressure conditions (at least 450 °C and 200 atm), the Haber-Bosch (HB) process is responsible for ≈1.44% of the global greenhouse gas emissions: ≈ 400 Mtons $year^{-1}$ of CO_2 released, with a global average of 2.86 tons of CO_2 emitted per ton of NH_3 produced, reduced to 1.6 tons of CO_2 per ton of NH_3 in the most efficient plants.[4] Currently, ≈ 465 000 metric tons per day (MTD) of NH_3 are produced worldwide with an energy consumption of ≈10 kWh kg^{-1} in modern plants; the production scale is at least 2000 MTD, but it reaches 6000 MTD in the most efficient ones.[4] Moreover, the HB process requires extra-pure reactants (i.e., N_2 and H_2) in a very precise proportion (1:3), and the N_2 production from air distillation (if air-fired secondary reforming is not used) is also energy-demanding due to the refrigeration temperature of ≈ −194 °C, besides the gas compression steps. Even using "green" or "blue" H_2, the HB process requires huge centralized plants to reach the highest energy efficiency (EE), which nowadays is ≈40%.[5] Thus, to achieve independence from fossil energy sources, it is vital to find a sustainable process carried out under mild conditions and driven by abundant, even if discontinuous, renewable energy sources.

In this scenario, the electrochemical N_2 reduction reaction (E-NRR) is under investigation as a renewable energy-based process for NH_3 production, representing a more sustainable approach than the well-established HB process.[6] E-NRR has the advantage of being displaceable and so adaptable to in situ production of high-value products (like fertilizers), even in remote areas, avoiding transport-related costs and emissions.[7] In addition, E-NRR strategies allow the delocalization of NH_3 production, since the efficiency of the process is independent from the plant scale, opening up the possibility of using renewable sources, i.e., wind or sun, to feed the process.[5]

A. Mangini, L. Fagiolari, F. Bella
Department of Applied Science and Technology
Politecnico di Torino
Corso Duca degli Abruzzi 24, Torino 10129, Italy
E-mail: federico.bella@polito.it
A. Sacchetti, A. Garbujo, P. Biasi
Basic Research Department
Casale SA, Lugano
Via Pocobelli 6, Lugano 6900, Switzerland

The ORCID identification number(s) for the author(s) of this article can be found under https://doi.org/10.1002/aenm.202400076

DOI: 10.1002/aenm.202400076

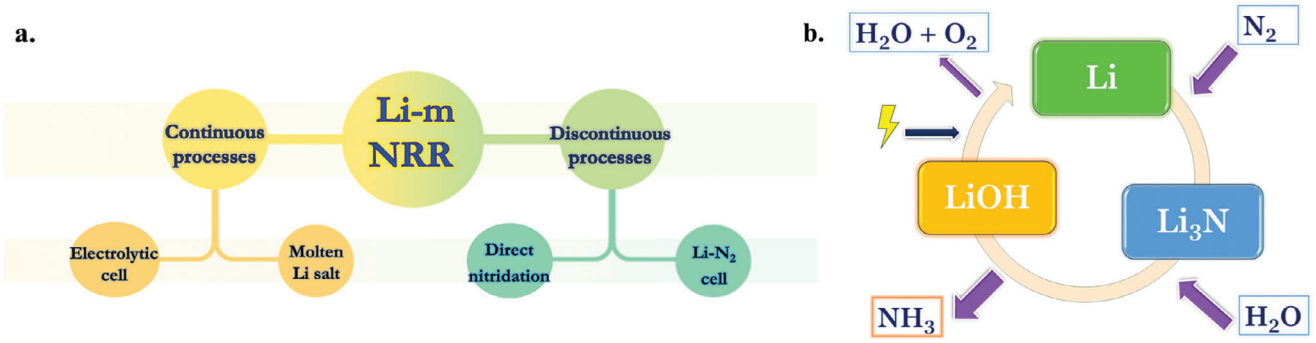

Figure 1. a) SoA overview of different Li-m E-NRR technologies: a systemic and synthetic classification. b) The three steps of Li-m E-NRR occur in discontinuous processes.

However, to become attractive as a scalable process, E-NRR has to obtain economic competitiveness in the market. In the REFUEL program of the Advanced Research Projects Agency–Energy,[8] the US Department of Energy stated that the threshold for the Faradaic efficiency (FE) at 300 mA cm^{-2} is 90% as the key performance indicator (KPI) of the process. To move toward this goal, the pivotal objective is the enhancement of selectivity. Another fundamental requirement from an industrialization viewpoint is an electric current density at least of 5–10 mA cm^{-2} for commercial NH_3 production.[9] It is correlated to the NH_3 production rate, a parameter as important as the FE and that should be more clearly considered in this research field.

Different steps must occur during the process: N_2 transport and absorption at the cathode and subsequent N_2 activation, with the triple bond cleavage, then the N_2 protonation to form NH_3, followed by NH_3 desorption and release. Generally, the achievement of KPIs is limited both by thermodynamic and kinetic factors, which favor competitive reactions, as will be discussed in the following section. In traditional aqueous electrocatalytic cells, the main competitive reaction is the H_2 evolution reaction (HER),[10] which limits the FE: the average FE value of recent findings is ≈ 20% for stable and reproducible catalysts.[5]

The energy efficiency (EE) of the whole system, rarely evaluated in the literature, should also be considered a valuable KPI for E-NRR processes, even if a correct comparison is essential to set proper and equal boundaries for the input and output calculation. At the current state of the art (SoA), it is hard to predict adequate information, and numbers based on general assumptions (instead of experimental data) could be misleading. An interesting methodology for this calculation takes into consideration the effective EE of the electrochemical reactor, calculated from the FE, and the overpotential necessary to drive the reaction. For cost-competitive NH_3 production, it has been calculated that the EE should be >30%.[11]

The stability in a long-term operating system represents a milestone toward a sustainable scale-up, necessary also to reduce the capital and maintenance costs.

Among the different electrochemical strategies developed in the last few years by the E-NRR community, the lithium-mediated (Li-m) approach has recently demonstrated promising results.[12,13,14] Li-m E-NRR may be exploited both in continuous processes, forming NH_3 in a single electrochemical cell,[15,16] and in discontinuous processes, involving a series of steps in different operating conditions, among which a fast Li_3N formation is the main challenge[17] (**Figure 1a**).

In the case of continuous processes, the Li-m strategy combines lithium use with the presence of a proton donor source, producing NH_3 in the same reactor and simultaneously as N_2 is activated. Starting from the landscape of the more traditional aqueous electrocatalytic cells for E-NRR, similar to CO_2 reduction cells and H_2O-splitting cells, a few studies tested the addition of lithium salt in the electrolyte.[18,19,20] In the aqueous case, the co-presence of Li^+ on the working electrode (WE) surface might both inhibit HER, thanks to a steric and repulsion phenomenon, and favorite N_2 activation.[18,20] However, the FE toward NH_3 is still far from 50%, and the production rate is very low. Recently, different research groups have obtained promising results with aprotic electrolytes, in which the controlled protons availability reduces HER.[21,22] Nevertheless, the organic electrolyte is easier to decompose at the operating potential. Key parameters that should be addressed in this field are the optimization of the proton source and concentration, in combination with the electrolyte reaction at the cathodic interface, and the study of N_2 and Li^+ diffusion rate toward the electrode surface.[23] Lithium has been tested in combination with both N_2 and H_2 and also in molten salt solution; a short dissertation is proposed also for this technology, even if the selectivity toward NH_3 resulted in limited and the technology is rarely further evaluated.[24]

In the case of discontinuous processes, the different reaction steps are separated in time or environment in order to enhance the selectivity and control of the process. N_2 is fixed in Li_3N without proton presence, thanks to the excellent reductive power of lithium, being completely exploited toward N_2.[10] Then, Li_3N is protonated exothermally and spontaneously into NH_3, while Li^+ has to be recovered and reduced into Li^0 (Figure 1b), which is essential and represents the most energy-demanding step.[17] In the direct nitridation strategy, N_2 gas directly and spontaneously reacts with metallic lithium, and the reaction is thermodynamically favored even under mild conditions, but the kinetic is insufficient for a mass-production process. The use of an electrochemical Li—N_2 Galvanic cell to reduce Li^+ could be an appealing solution to optimize lithium use and stabilize Li_3N.[25] This molecule is very reactive and environmental impurities have to be controlled.[26] Recent studies on those cells could open up new possibilities to boost the kinetics of N_2 fixation in comparison with direct nitridation, other than to recover the process

Table 1. Main issues of E-NRR processes and principal solutions.

Main E-NRR issues	Principal solutions
Thermodynamic stability of N_2 triple bond	Catalyst or mediator, such as lithium
HER competition	Control the amounts of protons source or avoid it during E-NRR in a stepwise process
Limited availability and mass transport of H^+ to the active site	Study on pK_a of the proton donor/carrier, study on hydrophobicity/hydrophilicity balance of the WE surface
Slow N_2 adsorption and activation kinetics, as well as NH_3 desorption	High specific surface area catalyst, study on the protonating acidic species
N_2 mass transport limitations	Use of a three-phase system, by-passing N_2 low solubility, or increase pressure
Components stability and sustainability: high maintenance costs	Closed-loop process with stable elements, full recycle of precious elements (lithium)
Detection limits: low product concentration, false positives	Straight protocol for testing (e.g., with constant gas volume) and analysis, final check with $^{15}N_2$ isotope labeling and NMR quantification
Infrastructure, equipment, and extremely pure reactant cost	Cooperation between research groups, straight and shared test and detection protocols

energy.[25,27] However, the reaction mechanism of Li_3N formation should be still clarified and, even in this cell, the cathodic interface should be optimized.[28]

In this review, the most significant achievements regarding different Li-m NH_3 production methods are summarized, discussed, and compared. Their limits and pitfalls are also analyzed to obtain an overall critical overview of the recent outcomes and to outline future outlooks in this emerging research field.

Firstly, the main challenges in E-NRR are discussed to give a general background of this field. The continuous Li-m strategies are then illustrated and the aprotic systems are deepened. The main parameters and KPIs are discussed in comparison to the traditional aqueous systems. A sub-section will also summarize works that approach the molten lithium salt strategy. Afterward, the multi-step discontinuous process is depicted with examples of direct thermochemical reactions between N_2 and metallic lithium, as well as the advantages and drawbacks of Li—N_2 cells. Finally, the main strategies described are compared, and an outlook on Li-m E-NRR scalability is given, closing with suggestions on the more urgent further implementations.

2. E-NRR: A Brief Overview of the Main Process Challenges

Besides thermodynamic issues, starting from N≡N triple bond stability and kinetic difficulties, as mentioned in the Introduction, other issues have to be tackled (**Table 1**).

The cell setup should be designed to guarantee the reactants' mass transport toward the reaction site. E-NRR depends on the co-presence of electrons, N_2, and H^+ at the interface of the conductive WE. N_2 is coming as a gas, ions are present in the liquid electrolyte, and the electrons are exchanged at the solid WE interface through charge transfer.[29] To ensure the three-phase contact, the use of gas diffusion electrodes (GDEs) in flow cells has recently emerged. The non-completely wettable WE interface and the study of particular hydrophilic/hydrophobic surfaces promote the contact between active sites, liquid electrolyte, and the N_2 gas diffusing from the gas chamber through the GDE microchannels, boosting the overall reaction.[21] The specific surface area exploitable for the reaction should be taken into consideration as a key parameter since it has to guarantee a high number of active sites.[21] The porosity and the morphology should be controlled, as well as the gas permeability and mechanical and electrochemical stability of the electrode. The main drawback of systems with GDE is the low probability of obtaining the correct co-presence of the three reactants at the solid–liquid–gas three-phase boundary, e.g. due to bubbles coverage of active sites, and stability issues such as flooding, also related to the salt-out and electro-wetting of GDE (see Section 4.1).[30,31] To simplify the system from a three to a two-phase reaction, there is the need to dissolve N_2 in the liquid electrolyte. However, N_2 solubility is insufficient in H_2O, and N_2 availability also represents the main limiting factor in organic solvents, even these latter are able to solubilize N_2 at least one order of magnitude higher than in aqueous systems.[32] It results that N_2 availability represents the main limiting factor for the production rate. The main strategies to overcome this issue are the application of high pressure (*e.g.*, 20 bar N_2) in E-NRR batch systems,[33] or the use of ionic liquids (ILs) as electrolytes. However, the most commonly used and already studied ILs for electrochemical processes present fluorinate anions,[34] which are characterized by uncompetitive cost,[35] or azo-compounds, which could lead to interferences and misunderstandings in the correct NH_3 quantification and origin.[36]

The main practical challenge for researchers working on this topic is an analytical issue, i.e., NH_3 quantification, since the amount produced in cells is lower or comparable with the detection limit for conventional NH_3 analytical detection methodologies. In addition, the contaminations coming from the environment, or from other nitrogenated components in the reactor, may create severe ambiguity about the real NH_3 production rate. The first studies in the E-NRR field used colorimetric methods or ion chromatography (IC) to quantify NH_3, but impurities, in particular coming from the N_2 gas feed, were not considered.[37] For this reason, when a pivotal Nature article was published in 2019, stabilizing a standardized straight procedure to assess the real NH_3 production,[38] many outcomes in this field were withdrawn or had to be revised. Afterward, many studies discussed how the origin of NH_3 in these experiments could also be identified as environmental contamination, e.g. impurities coming from the N_2 feed gas, but also from washed electrodes,

membranes, or even from the lithium salt purification process, and from the reaction of other nitrogen-containing molecules, easier to be hydrogenated.[36,39,40] The amount of NH_3 coming from all these contamination sources could be of the same order of magnitude or even exceed the expected NH_3 produced. So, it has become clear that the E-NRR process is too susceptible to false positives[40] and it requires very precise assessment procedures and gas purifications.[41] Among these, the cross-check of electrochemical experiments with $^{15}N_2$ isotope gas as a reactant and the subsequent nuclear magnetic resonance (NMR) analysis are needed to finally validate the obtained FE and NH_3 production rate. In this experiment, only the amount of $^{15}NH_3$ detected is accountable as the "true" reaction product, while any presence of $^{14}NH_3$ has to be assigned to impurities. Also, it is recommended to repeat the isotope labeling at different steps of the experiment to a better understanding of the process mechanism.[42]

However, recently some research groups have justified the absence of $^{15}N_2$-isotope cross-check asserting that the achievement of NH_3 quantity of the order of milligrams could exclude contamination influences.[43] Even in this case, degradation processes of azo-compounds used for example in the electrolyte should be straightly controlled for the purpose of a correct comparison with other studies, since these compounds could generate NH_3 that will boost the overall yield.

Apart from these validation requirements, research groups usually conduct E-NRR experiments using at least two detection techniques for routine verification of NH_3 production. The most common ones are colorimetric reactions, UV-visible analysis, and ionic chromatography analysis.

As regards colorimetric methods, the most applied ones are Nessler's reagent (NR), the Berthelot reaction with salicylates and cyanates, and the indophenol blue from phenol with hypochlorite.[44] All of these methods present some drawbacks, such as their sensitivity to pH range and to the stability temporal window of the photoreactive complexes formed. The NR also presents lower reliability at pH different from that of its medium and could also interact with cations different from NH_4^+, e.g. alkali metal ions, the presence of which as impurities in the sample is not often easily predictable.[45] The other mentioned methods present lower precision and are suitable only for high pH values.[46] An accurate quantification procedure with the salicylate method has been proposed by Giner-Sanz et al., but this procedure is optimized for aqueous samples.[47] In organic media, the NH_3 should be separated as NH_4Cl and the aprotic solvent should be evaporated, leading to practical difficulties for sub-ppm amounts.[47] Moreover, a further study from the same group pointed out the interference of alkali metal salt on the colorimetric chemicals.[48]

IC analysis has been recently applied by a few groups also in organic media. It presents many advantages, such as being less time-consuming and presenting a theoretically higher sensitivity, but a correct method and a suitable column have to be carefully assessed to avoid interferences with the electrolyte salt cations, the peaks of which could overlap the NH_4^+ one. Moreover, the instrumental compatibility with aprotic solvents should be verified.[49]

NMR is used by some groups for NH_3 quantification even without the isotope verification, although the costs correlated to this instrument would exclude it from routine analysis.[50]

Table 2. Comparison of metal nitrides that could be formed during electrochemical NH_3 production processes. Adapted and reprinted with permission from.[17]

Nitride	Nitride formation energy [eV]	Standard metal reduction potential [V]
Li_3N	−1.84	−3.04
Na_3N	+0.68	−2.71
Ca_3N_3	−4.0	−2.87
Mg_3N_2	−4.55	−2.70
Be_3N_2	−6.0	−1.85
TiN	−3.8	−1.63
ZrN	−2.6	−1.45
CrN	−0.5	−0.74

Another possibility is that of NH_3-selective sensors, but due to stability issues, such as surface fouling, they need frequent recalibration and maintenance.[51]

For low NH_3 amount detected, quantifications are usually supported with chemical-physical characterizations of reaction intermediate (as nitrogen-containing compounds present on the WE), e.g. X-ray diffraction (XRD), scanning electron microscopy (SEM) with energy-dispersive X-rays (EDX), or infrared spectroscopy (IR) analysis (as Fourier transform IR) of the WE itself (some examples will be presented in Section 5.2.1). However, the gas purification or isotopic labeling remains essential to demonstrate N_2 reduction and, due to the instability and sensitivity to air and moisture of the possible intermediates, in operando characterization should be considered to correctly and in situ identify intermediates, besides exploring the reaction mechanism. For example, XRD and IR measurements could be conducted in an ad hoc setup, as for CO_2 electroreduction studies.[52,53,54,55] The application of in-line gas chromatography-mass spectrometry (GC-MS), as well as differential electrochemical mass spectrometry, has been recently applied; however, calibration should be properly assessed since substances with a mass close to that of NH_3 could lead to ambiguous results.[56,57,58]

The importance of reproducible results, as well as validated with rigorous protocol, is truly high especially if the produced NH_3 is in the same range of possible impurities. With this aim, each FE value will be reported in this review article with a special symbol (i.e., FE*) if it has been verified with an NMR quantification of $^{15}NH_3$.[38]

3. Lithium Singularity in Spontaneous Nitridation

Lithium is able to form the most stable alkali-metal-nitride (Li_3N) and its formation is thermodynamically favored also under mild conditions,[17] thanks to its outstanding reduction potential of −3.04 V versus standard hydrogen electrode (SHE), as shown in **Table 2**. The activation energy to form Li_3N at ambient pressure and temperature (15.5 kJ mol^{-1}) is low in comparison with both the N_2 triple bond cleavage energy (410 kJ mol^{-1}) and with N_2H^+ formation enthalpy (ΔH^0 = 37.6 kJ mol^{-1}),[59] which is considered the rate-limiting step.[3] Finding a different pathway, with N_2 cleavage and Li_3N formation as intermediate, could enhance the production rate and circumvent the main inefficiencies

of the aqueous process.[60] Indeed, the Gibbs' free-energy variation (ΔG), which indicates the spontaneity of a reaction, is much lower for Li_3N formation ($\Delta G_{Li3N} = -154$ kJ mol^{-1}) than for NH_3 ($\Delta G_{NH3} = -16.4$ kJ mol^{-1}).[61]

In 1993, the reactivity of this alkali metal was investigated for NH_3 production in an aprotic electrolytic cell,[62] after the former dissertation by Fitcher et al. in 1930.[63]

Since the reaction between lithium and N_2 is spontaneous, the electrical current passage in the electrochemical cell is not necessary for this step, as mentioned in the introduction. For this reason, some studies separated the nitridation step from the others (lithium deposition and Li_3N hydrolysis). Pure N_2 reacts very fast with lithium surfaces; however, the reaction rate drastically falls down after a few minutes due to the formation of a Li_3N layer.[64] McFarlane and Tompkins observed that the process became pressure-dependent, suggesting that N_2 diffusion into the solid layer is the limiting step. Otherwise, at higher temperatures, the effect of pressure decreased, until the melting temperature of lithium (i.e., 180.5 °C) was achieved.[59] In the liquid state, N_2 diffusion was favored by lithium atoms motion and the reaction was no more pressure-dependent. Finally, the reaction between gaseous lithium and N_2 was generally excluded.[59] Modeling of metallic lithium by the density function theory (DFT) presents particular difficulties since lithium presents fluid-like structural fluctuations. Nevertheless, N_2 dissociation on the lithium body-centered cubic lattice, (110) surface, was studied and confirmed with metadynamics simulation between 300 and 500 K.[65]

Unoptimized lithium use could lead to an increase in the costs for its recovery, limiting the EE of the whole closed-cycle process.[17] Moreover, the use of metallic lithium will bring more safety concerns and the system should be designed in a perfectly sealed environment to avoid fast degradation with air and moisture.

The Li—N_2 reaction in an electrochemical cell could, instead, avoid the diffusion limiting step and optimize lithium exploitation: Li^+ migrated to the cathodic side may react individually with N_2 molecules, avoiding losses of unreacted lithium in the bulk and obtaining a higher production rate.

It is necessary to mention that lithium is entering the critical raw materials list: its abundance corresponds only to 10^{-3}% of the lithosphere composition, three orders of magnitude inferior to potassium.[66] Moreover, the lithium-based storage systems diffusion and exploitation are increasing, mainly through lithium-ion batteries (LIBs) and lithium metal batteries (LMBs) for electric vehicles. The development of Li-m E-NRR will use a closed cycle in which lithium recovery is an essential aspect and elemental losses estimation is 2%, which could be further optimized.[17] Furthermore, the broadly stressed literature on lithium systems from LIBs and LMBs allows a better understanding of the reaction mechanism in the electrochemical cell for E-NRR, as well as the pros and cons of the mediated pathway. Once an efficient Li-m process is well developed and comprehended, the substitution of this element with other alkali metals (e.g., sodium or potassium) could be considered to move forward to a more sustainable path.

4. Continuous Li-m Systems for E-NRR

In this section, the continuous strategies for Li-m NH_3 synthesis are detailed. In particular, electrolytic cells for E-NRR applying lithium addition are illustrated, and the main process parameters are discussed. After a short analysis of Li-m aqueous systems, the advantages of aprotic systems are highlighted. Finally, electrochemical strategies with solvent-free molten salts solutions, but operating at high temperatures, are discussed; a short digression on similar thermochemical strategies completes the panorama of Li-m NRR continuous processes.

As stated before, a focal point of this continuous technology is the co-presence of N_2 with H^+ at the WE interface, necessary for simultaneous N_2 activation and its protonation. Protons are supplied either from the addition in the electrolyte of a sacrificial proton donor or thanks to the coupling with H_2O electrolysis and a proton carrier that transports protons coming from the H_2 oxidation reaction (HOR) at the anode. The relative ratio between the three reactants is the fundamental parameter in order to obtain high selectivity and satisfactory performances. Currently, the best performances have been achieved with this approach, but some issues have to be fixed before targeting a scalable process.

4.1. Electrolytic Cell Architectures

Electrochemical cell design is an indispensable aspect impacting the process. The common architectures for E-NRR are based on multi-compartment batch or in-flow cells (**Figure 2**), similar to electrocatalytic H_2O splitting and CO_2 reduction processes. In batch cells, electrodes are immersed in an aqueous (Figure 2a-1) or organic electrolyte and N_2 is insufflated near the WE, or alternatively, the whole cell could be pressurized in an autoclave to obtain high N_2 saturation conditions. The homogeneous distribution of the reactants is aided by continuous stirring.[21,33,43,67] As represented in Figure 2a-2, in the two compartments H-type cell the anode and cathode are separated by a selective membrane (e.g., protons-exchange membranes), allowing, in some cases, even the co-presence of H_2O and organic electrolyte in the same cell (Figure 2a-3).[68]

Finally, in the flow cell equipped with a GDE (Figure 2a-4,5), the gas goes through the electrode and is in contact with the bulk electrolyte at the electrode surface, forming a three-phase boundary. The use of a GDE could be applied at the cathodic side (Figure 2a-4), but also at the anodic (Figure 2a-5), and both in aqueous and organic solvents. The latter is the case for a cell with HOR at the anode as a proton supplier.[69] The electrolyte is usually recirculated in the flow cell to ensure a convective mass transport of Li^+, H^+, and homogeneous reactivity on the WE.[69]

As the main advantage in comparison with a plain WE in a batch cell, the in-flow architecture with GDE ensures the availability of N_2 at the interface, overcoming the mass transport limitation of N_2 (Section 2), thus allowing the application of higher current density without losing in FE. Even if the process performances obtained in literature are not directly comparable due to the substantial differences between the two systems (e.g., the anodic reaction), the in-flow cell with the continuous replenishment of reactants opens to the scalability of the process.[70] However, the electrochemical and mechanical stability of the electrode itself is compromised due to competitive reactions: changes in wettability properties of GDEs could lead to flooding and consequent "salt-out", i.e., electrolyte crossing into the gas chamber and deposition on the back side of the WE, mining gas accessibility at

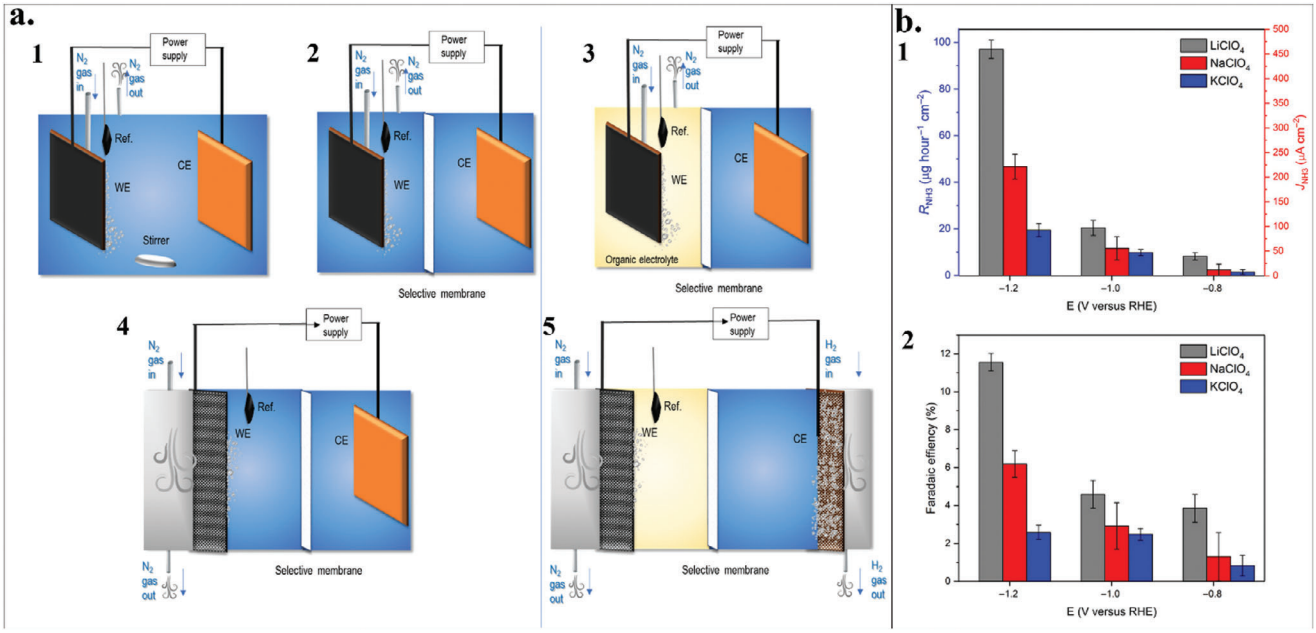

Figure 2. a) Different E-NRR cell architectures. On the left, aqueous systems: 1) single compartment batch cell; 2) two compartments static cell with a selective separator; 3) three compartments cell with GDE for the gas inlet in the cathodic compartment. On the right, cathodic compartments with organic electrolyte in combination with aqueous electrolyte for the anodic compartment: 4) two compartments system with selective membrane; 5) four compartments cell with two GDEs. b) 1) NH_3 production rate (R_{NH3}) and partial current density (J_{NH3}) measured at −1.19 V versus reversible hydrogen electrode (RHE), highlighting the effect of salt cations, i.e), perchlorate salts containing Li^+ (grey), Na^+ (red), and K^+ (blue). 2) Effect on FE. Chronoamperometry (CA) tests were conducted at −1.19, −0.99, and −0.79 V versus RHE in H-shaped electrochemical cells with an electrolyte molarity of 0.25 M. The best performances were achieved for Li^+ and dropped with increasing cation size. Adapted with permission from.[19]

the interface, as observed in CO_2 reduction tests.[71] Moreover, at the high cell potential needed, carbonaceous GDEs are mined by electro-wetting.[72] These issues are by-passed in the Li-m E-NRR setup since the application of an aprotic solvent requires a different material as GDE (i.e., a stainless steel cloth) to avoid Li^+ intercalation, and backpressure in the gas chamber contrasts the flooding (Section 4.5.1).[70,73]

The use of a membrane electrode assembly, as in CO_2 electrocatalytic reduction, is also under consideration to reduce solvent degradation and overpotential, even if the NH_3 production rate and FE are still limited in comparison with membrane-free systems (i.e., 41 ± 2 μg h^{-1} cm^{-2} and 9 ± 1% FE* at the cell voltage of 3.6 V).[74]

4.2. Li-m E-NRR in Aqueous Electrolytic Systems

In the last few years, a plurality of studies shared the ambition to find a process that could produce NH_3 under ambient conditions directly from H_2O and N_2 and in a continuous electrocatalytic cell.

Very briefly, the reactions occurring in the cell are H_2O oxidation at the anode, producing O_2 gas and H^+, which migrate at the cathode. There, these species combine (by different possible mechanisms) with nitrogen atoms adsorbed on a catalyst, so that N_2 is reduced to NH_3, the latter remaining dissolved in the aqueous electrolyte. The reactions are:

$$\text{Cathode side:} \quad 2N_2 + 12H_2O + 12e^- \rightarrow 4NH_3 + 12OH^- \quad (1)$$

$$\text{Anode side:} \quad 12OH^- \rightarrow 3O_2 + 6H_2O + 12e^- \quad (2)$$

$$\text{Overall reaction} \quad 2N_2 + 6H_2O \rightarrow 4NH_3 + 3O_2 \quad (3)$$

with $\Delta G^\circ_{NH3} = 339.3$ kJ mol^{-1}.[19]

As mentioned in the introduction section, the presence of a large amount of H^+ at the cathode produces H_2, due to its very similar onset potential to that E-NRR for each pure metal catalyst and its lower overpotential than E-NRR, other than the thermodynamically limitations of the N_2H species to be fully protonated into NH_2 and then desorbed as NH_3.[75] The use of a selective catalyst and a designed electrolyte could, however, enhance FE toward NH_3. Most of the studies focus on the catalyst nature and morphology; however, generally, FE remains under 10%, only a few of them exceeded this value and with very low current density and/or not accompanied by proper straight gas purification and results validation protocol.[18,76,77] Recently, outstanding performance employing BiO_2 as a catalyst has been obtained, but controversy is ongoing on this material.[78,79,80]

It should be said that H_2 coming from E-NRR could anyway be considered a value-added product, but process-related figures of merit (e.g., cell costs and EE) are less competitive than those already present in the market; the main issue here is that current technologies are not optimized for reducing both H_2O and N_2, thus in the E-NRR scientific community H_2 production is not considered as an advantage.[5]

A peculiar example is the process proposed by Hollevoet et al., in which purified N_2 for E-NRR is produced from the combustion of the unwanted H_2 in the outlet stream with the O_2 present in

the air in-flow, consuming it before entering into the process. In this way, they would operate with humid N_2 without any air separation step. The main limitation of the scale-up was evaluated to be the current density, which was still far from 5–10 mA cm^{-2}, i.e., the value suggested for commercial NH_3 production.[9]

The presence of solvated alkali metal ions, as a salt in the electrolyte, has been found to constitute a steric barrier to H^+ at the cathode,[78] enhancing selectivity toward N_2 molecules reduction. Thanks to the previously discussed behavior of lithium toward N_2, also in aqueous system the presence of lithium in the electrolyte or in the WE surface presents a destabilizing and catalytic effect on N_2 chemisorption, as DFT studies confirmed.[20,65,81]

Guha et al. tested a concentrated lithium salt (i.e., $LiClO_4$ 5 M) in a three-compartment aqueous electrolytic cell and demonstrated the onset potential dependence on salt concentration.[20] A higher concentration of lithium salt involves a higher amount of H_2O molecules to solvate ions, as explained in the "H_2O-in-salt" concept electrolyte already developed for LIBs,[82] suppressing HER on the WE surface. Therefore, by increasing the salt concentration from 0.1 to 5 M, they were able to carry out E-NRR at a higher potential ($^-$1 V instead of $^-$1.15 V vs. Ag/AgCl) with copper as WE, thus overcoming the onset potential of HER ($^-$1.1 V vs. Ag/AgCl).[20] They observed an increase in the current density addressed to the reaction, from 0.07 to −0.3 mA cm^{-2}_{geo} (i.e., considering the geometric surface area). This observation could be correlated to the improved conductivity of the electrolyte and the higher availability of reactants.[20] With this setup, the best result obtained was quite good for an aqueous system, with a FE of 12% and an NH_3 production rate of 12 ± 2 μg h^{-1} cm_{geo}^{-2}.[20] The same authors repeated the tests with gold as WE material and observed how the WE nature is another critical parameter for performances: gold, usually a benchmark for reduction processes in electrolytic cells, further enhanced HER instead of E-NRR.[20] Moreover, DFT calculations showed that neither copper nor gold should present high activity with N_2 since the binding energy of these metals with N_2 is negative (e.g., $\Delta E_{Cu\text{-}N2} = -0.23$ eV) and the N_2 triple bond could not be broken in this setup in absence of lithium, which is supposed to elongate the N_2 bond distance from 1.12 to 2.91 Å. The tests have shown undoubted advantages with respect to experiments carried out with $NaClO_4$, which did not show any NH_3 production under the same conditions.[20]

Similar results have been achieved by Zhao et al.[83] and by Song et al.[19] with $LiClO_4$ 0.1 and 0.25 M, respectively. In the first case, the high FE achieved (12.5%) supported the authors' hypothesis that the C–O functional group of the oxidized carbon nanotubes (i.e., the active material at the WE) may be critical for the reaction, with a strong absorption energy toward N_2 molecules of −0.32 eV, calculated by DFT. At −0.4 V versus RHE in a two-compartments cell, an NH_3 yield of 32.33 μg h^{-1} mg_{cat}^{-1} was reported.[83] A favorable interaction between N_2 and Li^+ associated with oxygen atoms-rich catalysts was also suggested by Wang's group.[84] Song et al. achieved an FE of 11% at −1.19 V versus RHE and a production rate of 97 ± 7 μg h^{-1} cm^{-2}, with encouraging stability for ≈ 100 h. They also calculated the system EE, equal to 5.25%. In this case, the authors supposed that the key factor of the system is the nanospike-shaped working electrode, able to enhance the electric field and current on the active sites and promote E-NRR.[19] As shown in Figure 2b, when comparing different alkali metal perchlorate salts, the performances dropped while increasing the cation size, confirming that lithium presence is a key factor. A possible explanation was the HER suppression thanks to the local pH rising at the surface: the pH unavoidably changes during an E-NRR experiment, and the effects on the systems, such as NH_3 migration to the anode, are not yet deeply evaluated.[19,85]

Liu et al. obtained comparable performances combining MoS_2 nanosheets catalyst with 0.1 M Li_2SO_4 electrolyte, with NH_3 yield rate of 26.8 μg h^{-1} cm^{-2} and FE* of 10% at −0.2 V versus RHE. They demonstrated tenfold increasing performance in comparison with $NaSO_4$ 0.1 M, thanks to Li-S interaction, proven both experimentally and through DFT calculations.[18] The combination of iron and molybdenum as catalysts and a lithium salt has been considered too, both by DFT study and experimentally, obtaining an FE of 27% at −0.05 V versus RHE.[86]

Most of the reported experiments with lithium salt presented performances with superior respect to other aqueous E-NRR systems.

Lithium has been tested even as dispersed active sites in the catalyst: Gu et al. suggested the synergic catalyst composed of $LiFeO_2$ onto reduced graphene oxide. This active material, in combination with an electrolyte based on Na_2SO_4 0.1 M, gave an NH_3 yield of 8.1 μg h^{-1} cm^{-2} and an FE of 16.4% at −0.3 V versus RHE.[87] Similar results were obtained with a $LiMo_2O_4$ catalyst,[88] but in that case, results were not validated by isotopic labeling. Since the mentioned results do not outperform the average figures of merit of non-lithium metal catalysts, it is not possible to claim lithium as a key element in (electro)catalysts; conversely, its presence in the electrolyte is decisive.

To summarize, the advantages of lithium as the salt cation in comparison to other alkali metal cations have been proven in aqueous media for the Li-m E-NRR, but it seems insufficient to enhance the selectivity toward NH_3 due to HER and the direct protonation of lithium. Even the combination with particular morphology or oxidized cathodic material appeared determinant.[19,83] Up to date, the use of a continuous electrolytic cell with aprotic solvent is more extensively evaluated for Li-m technologies. In the future, if a scalable effective technology is developed for HER suppression, the aqueous environment could be evaluated again for an even more sustainable process.

4.3. Li-m E-NRR in Aprotic Electrolytic Systems: Fundamentals

All these findings have led the Li-m E-NRR research to move from an aqueous environment to aprotic solvents, nowadays widely studied in the LIBs field.[89] As mentioned in Section 4.1, Fitcher was the first to check the possibility of performing Li-m E-NRR in 1930.[63] Tsuneto et al. experimentally investigated the process for the first time in 1993 in a pressurized electrolytic cell with a lithium salt, different metallic working electrodes, and H_2O or EtOH as proton donors, establishing $LiClO_4$ 0.2 M and EtOH 1 vol% in tetrahydrofuran (THF) as the best electrolyte formulation.[62] Sakata et al. 1994 carried out their experiments, and EtOH 0.18 M (or 2-propanol) in THF was observed as the best proton donor.[15] From these results, EtOH has been selected as a standard source of protons for NH_3. In recent years, Andersen et al. were able to reproduce Tsuneto's work and performed Li-m E-NRR in the same aprotic system with a controlled gas

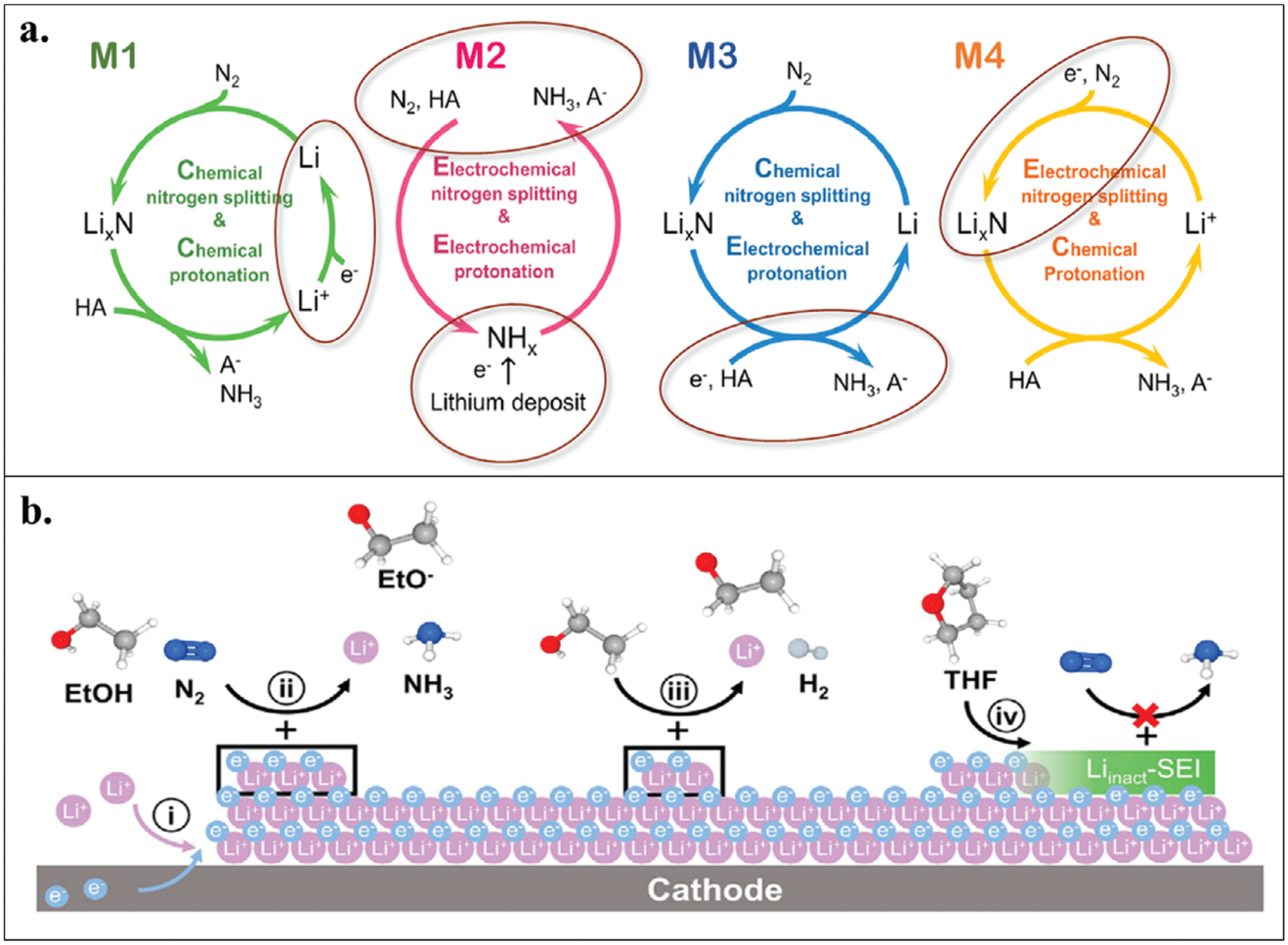

Figure 3. a) Li-m E-NRR possible different mechanisms. The elliptical circles highlight the electrochemically driven steps. From the left: M1) with both chemical N_2 splitting and protonation; M2) with both electrochemical N_2 splitting and protonation; M3) the mix of the previous two models, with chemical N_2 splitting and electrochemical protonation; M4) vice versa, i.e), combination of electrochemical N_2 splitting and subsequent chemical protonation. Adapted and reprinted with permission from.[91] b) Illustration of the mechanism of Li-m E-NRR, in which four dominant phenomena seem to occur: i) electrodeposition of Li^+, ii) chemical N_2 splitting and NH_3 synthesis, iii) chemical H_2 evolution, and iv) passivation of metallic lithium via reaction with electrolyte) Adapted and reprinted with permission from.[91]

purification protocol and verified the outcome through NH_3 isotope labeling;[22] in parallel, mechanism understanding was provided by Lazouski et al.[16] The development of the HB process in 1911 slowed down the research on the topic,[90] but nowadays the climate crisis urgency has made the electrochemical system based on THF and "lithium cycling" be in vogue again. In these studies, the term "cycling" has been used since lithium, applied in a consistent amount to fix N_2, assists its reaction with protons, and then it is recovered at the end of the reaction. Nearly constant availability of this mediator is maintained in the system.

4.4. Li-m E-NRR in Aprotic Electrolytic Systems: Mechanism and Parameters

The exact reaction pathway is still unclear and under study. Up to date, two main hypotheses have been supported as reliable (i.e., M1 and M2 in **Figure** 3a), but also different combinations of the proposed reaction steps are under evaluation (i.e., M3 and M4 in Figure 3a).[91] In all cases, the fast and unique kinetic of the chemical lithium nitridation holds the intrinsic advantage of the Li-m pathway.[22]

In the first mechanism (i.e., M1 in Figure 3a), Li^+ species are electrochemically reduced at the cathode into lithium metal (lithium deposition or plating), then lithium fixes N_2 to form Li_3N (nitridation). The latter is predicted to be the rate-determining step, and it is followed by fast Li_3N protonation into NH_3, closing the lithium cycling.[92] In this case, only lithium plating is an electrochemical reaction, and N_2 activation and protonation are chemical reactions that do not require electrical current. N_2 reduction is aided by the presence of lithium, deposited on the WE, and "storing" the electrons of the imposed current necessary for N_2 reduction. The reaction steps are exemplified for the case in which EtOH is applied as a proton donor:[52]

$$Li^+ + e^- \rightarrow Li \qquad \Delta G = 293\ kJmol^{-1} \qquad (4)$$

$$6Li + N_2 \rightarrow 2Li_3N \qquad \Delta G = -135\ kJ\ mol^{-1} \tag{5}$$

$$Li_3N + 3EtOH \rightarrow NH_3 + 3Li^+ + 3EtO^- \qquad \Delta G = -760\ kJ\ mol^{-1} \tag{6}$$

The second step (eq. 5) competes with direct lithium protonolysis:

$$Li + 2HA \rightarrow Li^+ + 2A^- + H_2 \tag{7}$$

A schematic representation of M1 on the WE is reported in Figure 3b.

In the second mechanism (i.e., M2 in Figure 3a), an associative pathway is proposed to occur on the lithium surface. In this case, after the electrochemical Li^+ deposition at the cathode, N_2 is chemisorbed on lithium or on $Li_xN_yH_z$ species formed on the WE interface. After the triple bond elongation, H^+ protonates N_2 with a coupled proton-electron transfer assisted by the electrolytic cell, in a completely electrochemical process, similar to the most common mechanism described for aqueous systems. Finally, NH_3 is formed and released, leaving lithium active sites free and closing the local lithium cycle.[91] Even in this case, N_2 fixation competes with lithium protonolysis, but is still uncertain if the formation of lithium-based secondary products could itself be beneficial for E-NRR, forming some species able to activate N_2, such as a $Li_xN_yH_z$ layer, and able to open up a pathway with a chemical-looping reaction.

Differently, M3 hypothesizes a combination of chemical N_2 fixation on the $Li/Li_xN_yH_z$ species on the cathode and an electrochemical protonation of adsorbed nitrogen atoms.[22] Finally, M4, with electrochemical Li_3N formation, is the mechanism proposed for Li—N_2 batteries, in which this product of interest should be formed before lithium plating, at a higher potential, and its protonation happens in a subsequent step, chemically. This process will be deepened in Section 5.2.

The fully electrochemical mechanism (M2) has been put under discussion by Cai et al.: they tested Li^+ deposition both under N_2 or argon atmosphere, then insufflated N_2 in the electrolyte without any applied current, and NH_3 was formed in both cases. Moreover, the electrical current variation from N_2 to argon during Li^+ deposition was negligible, and the final NH_3 amount produced was similar.[91] Even in the absence of EtOH during Li^+ plating, but flowing consecutively with both N_2 and EtOH under open circuit rest conditions, NH_3 was produced. On this basis, this study refuted the necessity of applied current for N_2 splitting on lithium in the cell.[91] As explained in Section 2, the reaction of lithium nitridation as well as its protonation is, indeed, spontaneous.

It can be concluded that the only step that is well recognized as electrochemically driven in the electrolytic aprotic system is the lithium plating on the cathode. The current density influence on the selectivity is crucial for an efficient and stable process, and the mechanism should be deeply indagated. Moreover, it is probable that, with different parameter settings, the favorite mechanism between M1-4 would change.[93] The kinetic rate-limiting step is hard to identify since it is hidden by other limiting factors, such as the mass transport limitations of the reactants on the active site.

The ratio between the three reactants necessary for NH_3 production on the WE interphase is evidently crucial for each mechanism. N_2, protons, and Li^+ on the WE active sites have to maintain an equilibrium in this complex system to guarantee the desired reaction to happen with a high selectivity and to maintain the system stable.

Reactant ratio boundaries have been first proposed by Andersen et al., who calculated them employing a kinetic-transport model, as shown in **Figure 4a**.[22] The ratio between N_2 and proton concentration, $r(N_2/H^+)$, should follow the stoichiometry of NH_3 to develop this molecule at the interface, so the protons' amount in the electrolyte needs to be maintained as high as $r(N_2/H^+) > 1/6$, as outlined by the dashed green line in Figure 4a.

As explained in Section 2, N_2 is usually the main mass transport limited reactant on the WE surface. As a consequence, the proton amount should follow a trade-off strategy;[69] a threshold for the optimum amount of protons, for high performances, should thus be defined. A high amount guarantees easily available protons, accelerating the reaction rate, but, on the other hand, protons might also react directly with lithium, causing the mediator depletion or the formation of competing products such as LiH, H_2, and LiOH, lowering the FE.[92,94]

Moreover, the amount of freshly plated lithium, as well as the one of active lithium at the WE, are also evidently critical to optimize FE. Despite the high reactivity of lithium being a desired quality for N_2 fixation, the plated lithium at the interface leads to the formation of sub-products due to the interaction with the other components of the system. Indeed, at the severe voltage needed for lithium plating, the decomposition of the organic electrolyte at the interface is unavoidable and driven by the polarization of the cell. Even if a high current is necessary to increase the NH_3 production rate, excessive lithium deposition could lead to electrolyte destabilization, with the consequence of FE fading and electrolyte depletion in secondary difficult-to-predict organic sub-product.[91]

Moreover, in aprotic system the reactive interfaces of electrodes are passivated by a spontaneous reaction of the electrode with the electrolyte, forming an unavoidable layer called solid electrolyte interphase (SEI). This layer has been widely proven as essential for metallic lithium passivation from secondary reactions in LIBs.[95] It could represent a beneficial protective element that ensures stability and controls reactant transport, but also a resistive detrimental factor. This layer is more and more emerging as a key element for reaction boosting: the reaction rate is strongly influenced by its permeability by each reactant and by the catalytic effect of the species it is formed.[96] Even with a minimal amount of a different reactant or additive, it may change its composition, thickness, resistivity, porosity, and durability.[97] The SEI layer composition in LIBs is tailored principally by varying the chemistry of the electrolyte. As in the battery sector, the Li^+ solvation shell should be tailored to be easily reduced on the WE, thus forming a stable inorganic passivating layer, that will avoid further degradation of the electrolyte (i.e., the so-called formation step).[98]

The nature of the proton donor itself determines the formation of different interfacial species on the WE and reaction pathways.[93] Recent studies showed that EtOH is essential not only as a proton carrier but is specially required to ensure the formation of a SEI layer able to be easily penetrated by N_2.[99]

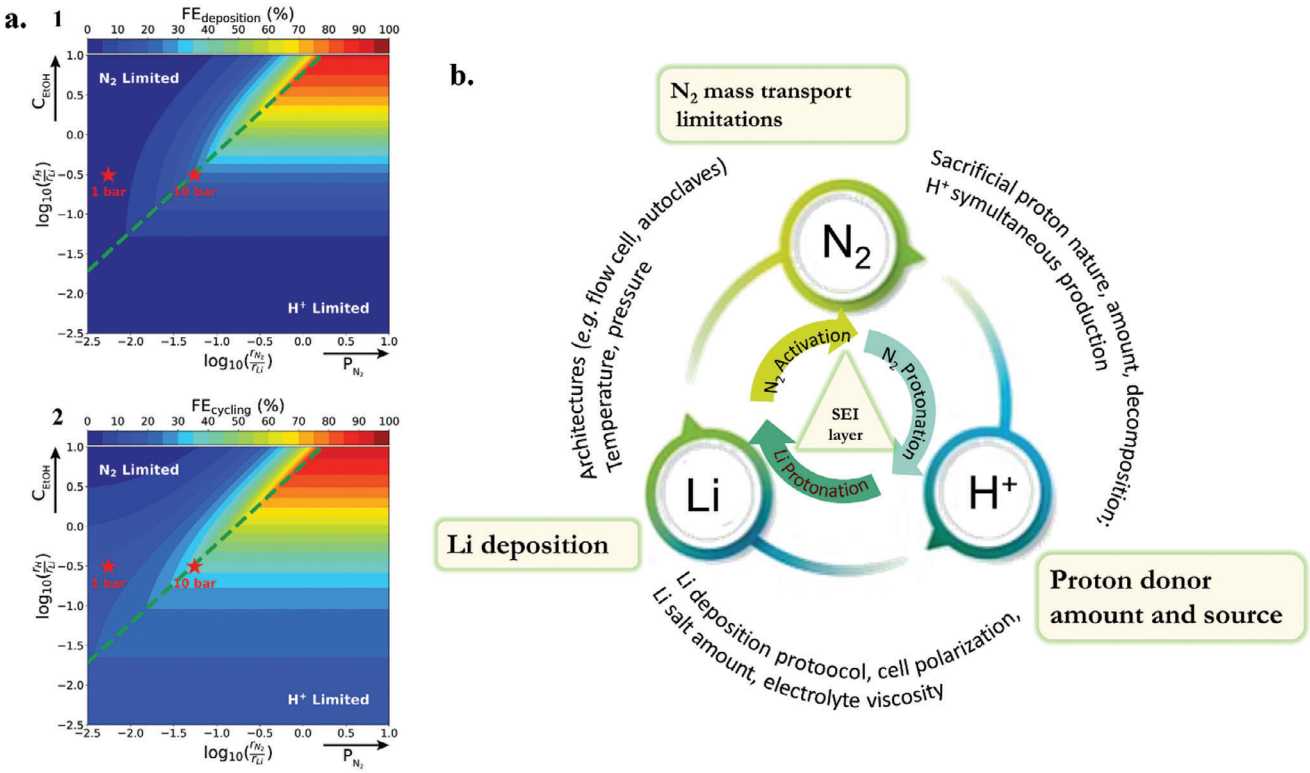

Figure 4. a) Heatmap of the predicted FE as a function of the N_2 over lithium ratio (x-axis) and proton over Li^+ (y-axis) diffusion rates: 1) FE during constant lithium deposition; 2) FE during electrolysis test with "cycling protocol", with current application alternated to rest period) The dashed green line indicates the boundary between regimes of N_2 transport limitations (upper left) and H^+ transport limitations (lower right). Adapted and reprinted with permission from.[22] b) Factors and parameters affecting the E-NRR process.

In the next section, the limitations, parameters, and correlated phenomena are described in detail for each of the reactants, i.e., N_2, Li (including Li^+ and electrons), and H^+. It is necessary to mention that, differently from aqueous systems, each component of the cell plays a key role in the aprotic system, and so each of them will be analyzed as well. The solvent, the proton donor or carrier, the anion, and even small amounts of impurities could greatly influence the FE, since they could lead to a different reaction pathway, and could modify the composition or morphology of the SEI layer on the WE surface.

As resumed in Figure 4b, the main factors correlated to the three principal reactants and influencing stability and KPIs could be summarized as follows:

- N2 transport limitations to the WE, depending on the different cell architectures.
- Lithium plating protocol is related to lithium deposition rate, and so to the electric current density, which directly determines the system polarization and the SEI layer formation.
- The amount and chemistry of a sacrificial proton donor or carrier correlated to parasitic reactions such as HER and electrolyte decomposition.[100]
- The electrolyte chemistry, in terms of solvent and anion nature, lithium salt concentration, impurities, and their different combination in the SEI layer.

Each of these species is related to the other and determines the overall cell performance.

4.5. Li-m E-NRR in Aprotic Electrolytic Systems: Cell Components

4.5.1. N_2 Transport to the WE in Different Architectures

The majority of the Li-m THF-based systems are single or two-compartment H-type cells with continuously stirred liquid electrolytes, saturated with N_2 (Section 4.1).[21,33,101] The gas can be both bubbled at ambient pressure or, to have sufficient N_2 dissolution in the electrolyte, autoclaved cells (up to 20 bar) have also been explored.[15,22] Chronopotentiometry (CP) tests with 1.1 mA cm^{-2} at 3.8 V versus Ag/AgCl, in a two-compartment cell with $LiClO_4$ 0.5 M in THF, revealed that lithium reaction with N_2 on a molybdenum WE under 10 bar of N_2 is still limited by N_2.[16]

The alternative is the in-flow architecture with GDE WE, in which the three-phase contact should guarantee higher N_2 transport to the active site and consequently higher NH_3 yield. This structure is still rarely considered in the literature, but it is interesting for coupling E-NRR with HOR at the anode for continuous protons feeding into the system.[69] Lazouski et al. studied the flow cell architecture in combination with different N_2 pressure values in the WE chamber. In that study, the behavior

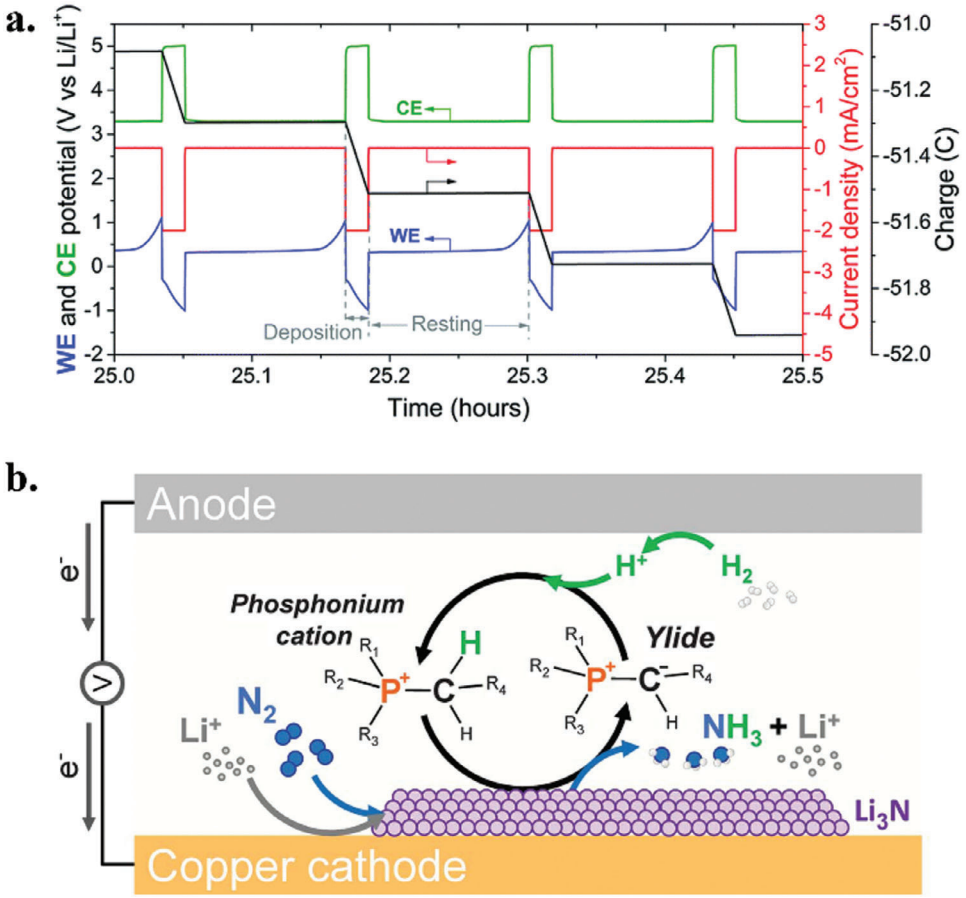

Figure 5. a) "Potential cycling" methodology: the imposition of the electric current (2.0 mA cm^{-2}) necessary for lithium plating is alternated to a rest step (i.e., 0.0 mA cm^{-2}). The graph represents the imposed electric current (red line), the measured WE and counter electrode (CE) potential versus Li^+/Li (blue and green lines), and the total charge accumulated in the system (black line). Adapted and reprinted with permission from.[22] b) Phosphonium shuttle effect mechanism proposed in.[102] The [P](eFAP$^-$) complex is able to transport a proton from the anode of the electrolytic cell, where HOR happens and H_2 is oxidized into H^+, which reacts with the phosphonium cation forming the ylide, subsequently migrated to the cathode, where H^+ is essential to protonate Li_3N into NH_3 and Li^+. Adapted and reprinted with permission from.[102]

and wettability of different materials were analyzed and stainless steel (SS) was observed to guarantee greater free specific areas for tri-phase co-presence in comparison to carbon fiber supports.[73]

4.5.2. Current Density and Li Deposition Protocol

The amount of plated lithium depends on the current density. Indeed, lithium deposition requires the simultaneous presence on the WE surface of Li^+ from the electrolyte and electrons from the WE. The ionic transport is correlated to the viscosity, the solvation of Li^+ in the electrolyte, and the presence of eventual separators (influencing the ion transport number).[98] Conversely, the electrons' presence is correlated to current densities and electrode resistivity. As previously explained, high current density is required to satisfy industrial-scale requirements. On the other hand, if the current density is not correctly proportioned with the N_2 activation kinetics, an increasing number of electrons at the WE interface could destabilize the process. Indeed, an exceeding lithium plating rate will increase thickness and inhomogeneity of the lithium layer on the WE and its reactivity with other elements in competitive reactions. Hence, the overlapping of many irregular or dendritic lithium multi-layers may prevent its complete utilization, lowering the FE. Moreover, the WE polarization could generate a potential value at the interface higher than expected, which could exceed the electrolyte stability window.[92] It has been experimentally observed that a disproportionally high lithium plating rate on a molybdenum WE leads to the formation of a multi-layer structure and a thicker SEI layer in a single compartment cell employing $LiClO_4$ 0.3 M and EtOH 1 vol% as electrolyte and at 10 bar of N_2.[22] To bypass this issue, a specific testing protocol alternating the high voltage periods of deposition with rest periods was designed for this system, called "potential cycling". With this "potential cycling" protocol, authors were able to increase the EE up to 6.9 ± 0.5% and the FE* up to 37 ± 1%.[22] The CP time was set as short as is necessary to prevent the WE drifting due to polarization (**Figure 5a**).[22] When switching to resting, the WE potential immediately turns to just above 0 V versus Li^+/Li and, after a short time, the WE increased more, suggesting the dissolution of deposited lithium species. At this point, another lithium deposition pulse is applied. The alternated CP/rest periods allow

lithium at the cathode to react with N_2 in the rest phase, preventing accumulation and maximizing the exploitation of the "reservoir" of deposited lithium. Due to this "lithium storage" effect, the authors named the system a "pseudo-battery". The stability was observed to increase after 125 h with a total FE of 21%.[22]

4.5.3. Protons Sources

Amount and Chemistry of the Proton Donor: As explained in Section 4.4, a trade-off is needed to find the optimal proton concentration or the reaction would be proton-limited. At the same time, HER should also be suppressed.[69] The impact of protons concentration on the system stability was observed experimentally: lithium plating is notably reduced and overcome by HER and SEI layer thickening if EtOH amount exceeds 5 vol% in THF in a stirred batch electrolytic cell. The surface passivation, assessed by electrochemical impedance spectroscopy technique, increased in correlation with the EtOH amount: at high EtOH amounts, the internal resistivity increased, as well as without EtOH, indicating the formation of species in the SEI layer being not suitable for the process.[92] Moreover, without EtOH, the WE surface after test was observed flatter and covered by a less penetrable SEI layer, supposed to inhibit lithium nitridation, as studied by cryo-electron microscopy.[103] The degradation of EtOH during the SEI layer formation could indeed inhibit the THF polymerization.[99] On the other side, an excess of organic components in the SEI layer could mine its mechanical stability. An unstable even if porous SEI could prevent long-term operation of the process, due to continuous electrolyte degradation at the interface.

It is necessary to mention that the reaction intermediate Li_3N is very unstable, and its protonation rate should be carefully assessed for an efficient E-NRR system. The thermodynamic study suggested operating at low EtOH concentration to favor a stable Li_3N layer with respect to LiH. A DFT model of the Li_3N surface layer suggested that the stability of the compound is correlated to the vacancies in the crystalline structure of deposited lithium, which could stabilize Li_3N and guarantee its correct and fast protonation by available H^+ in the electrolyte.[92] At the same time, if the vacancies on plated lithium surface diffuse into the lithium bulk, they could destabilize the Li_3N structure. Eventually, HER and lithium dissolution could predominate over NH_3 formation in this competitive environment. Therefore, a very fast proton transport could reasonably lead to lower selectivity. This consideration is coherent with the phenomena occurring with the nitrogenase enzyme, which works in an anaerobic environment where the proton transport is slow, obtaining a FE of 75% (an isotope test was not presented, but the authors claimed to have performed it for previous studies in the same laboratory).[92] In a batch cell, a compromise of 1 vol% EtOH was mainly applied,[92] but the optimal value decreases to 0.25 vol% in presence of HOR at the anode in flow cells.[69]

Even if EtOH showed appropriate properties for Li-m E-NRR, the depletion, and shortage of this molecule, both if it is used as a proton donor or as a carrier, should be assessed for a stable continuous process. Moreover, its cost and fossil fuel origin have to be considered, and a more sustainable proton carrier should be studied for a circular system.[16]

The more profitable sacrificial proton donor toward N_2 protonation has been predicted with artificial intelligence and machine learning. The ability to donate a proton was calculated starting from thermodynamic laws, then a classification model was studied to categorize different organic molecules for their donating ability.[104] To achieve this goal, the hydrogen-bonding donating and accepting properties of many compounds were predicted from the solvatochromic Kamlet-Taft parameters.[104] The study was compared with experimental tests in a two-compartments cell with an SS-flooded cathode in $LiBF_4$ 1 M in THF.[100] Linear aliphatic alcohols emerged as the best species able to ensure an active surface and a stable SEI layer; in particular, 2-propanol resulted in the best option from the model, followed by EtOH, 1-butanol, and aliphatic poly-alcohols. The optimal concentration was confirmed to be ≈ 0.1 M (≈0.6 vol%) for EtOH and between 0.1 and 0.6 M for other proton donors.[100] Interestingly, Lazousky et al. observed that the presence of the proton donor from the beginning of the experiment, as well as the order of addition of the reactants in the process, are factors determining the FE. Tests assessed in single-compartment THF-based electrochemical cells achieved higher performances only in co-presence of all the reactants (N_2, Li^+, and the proton donor) from the beginning.[100] This observation disagrees with the idea of differentiating the three reaction steps in a discontinuous process (lithium deposition, then N_2 flow, following the proton donor addition), described in Section 5. As mentioned before, the reaction is still uncertain and the system is very complex; the variation of each parameter could lead to very different results, bringing alternative pathways.

Electrolytic Cell Symbiosis: H_2O Splitting + E-NRR with HOR: To avoid the consumption of a sacrificial organic compound acting as a proton donor, researchers are moving to the combination of HOR at the anode with a proton carrier in the electrolyte.[73] Moreover, this option avoids THF oxidation, polymerization, and consumption. However, even in this case, a proton source is required in the cell, not resolving the pure H_2 feed need, which could be ensured by a more traditional H_2O-splitting electrolytic cell.[73]

The carrier should be able to transport H^+ from the anode, where the just oxidized H^+ is bounded, to the cathode, where the proton is released for E-NRR, allowing the so-called "shuttle effect". An interesting proton carrier is a phosphonium salt with the phosphonium tris(pentafluoroethyl)trifluorophosphate ($eFAP^-$) anion, which is also able to increase N_2 solubility (Figure 5b). This ylide enabled high NH_3 production rates (32.5 ± 0.6 μg h^{-1} cm^{-2}) and a FE* of 69 ± 1% in 20 h of experiment under 0.5 bar H_2 and 19.5 bar N_2, and ensured stable continuous process up to 3 days.[102]

In comparison with EtOH or proton donors in general, the proton carrier methodology was demonstrated to enhance the stability of the cell. The addition of a proton acceptor (the carrier) could, moreover, stabilize protons in the system as in a buffer solution, obtaining a more stable chemical potential.[94] Even EtOH could be applied as a proton carrier instead of as a sacrificial proton source, maintaining its crucial role in the SEI layer formation.[99] Moreover, a carrier such as the phosphonium salt seems to be unable to lead to a very high FE due to the formation of an unfavorable resistive SEI layer, confirming the importance of organic short-chain components in this layer.[93] With an SS GDE in a three-compartment cell, and $LiBF_4$ 1 M and EtOH 0.11 M in THF

electrolyte, an NH_3 partial current density of 8.8 ± 1.4 mA cm^{-2} and an FE of 35 ± 6% were obtained.[73] The EE was suggested to be theoretically optimized at 26% thanks to the resultant minimized overpotentials of Li-m E-NRR cells.[43]

HOR was assessed in combination with lithium bis(trifluoromethylsulfonyl)imide (LiTFSI) and dried THF on a highly dispersed Pt/C-supported catalyst, but the low potential needed for E-NRR has been observed to deteriorate the catalyst for HOR at the anode and even in this case the process should be optimized.[105] Other catalysts for HOR are under evaluation, such as Pt/Au, with promising results. On the other hand, platinum presence, besides enhancing the overall process cost, would require the absence of sulfur-containing compounds or impurities, or the catalyst would be deactivated.[69]

H_2O should be the most preferable proton source, but, even in low amounts (hundreds ppm), it has been demonstrated to have mainly negative effect in the aprotic system, as will be illustrated in the next paragraph, due to promotion of organic electrolyte degradation.[16]

The two approaches (i.e., aqueous and aprotic) were also tested in a two-compartment cell, in which the two different electrolytes (i.e., aqueous and aprotic) were separated by a cation exchange membrane.[68] On one side, a lithium salt was used for E-NRR on the cathodic WE in the aprotic solvent environment ($LiClO_4$ 0.1 M in ethylenediamine). The consumed reactants as H^+ were regenerated in an aqueous environment, using H_2O as a proton donor, without organic solvent decomposition. In this case, the O_2 evolution reaction could be the rate-limiting step and other acidic solutions should be chosen (e.g., H_2SO_4 0.05 M).[68] A NH_3 production of 2.2 μg h^{-1} cm^{-2} was obtained at a cell voltage of 1.8 V. Ethylenediamine has been chosen for its stability toward reduction, but its degradation could still develop false positive results, even at the anodic side because of solvent crossover through the membrane. These membranes, moreover, present high cost and maintenance needs.

4.5.4. Electrolyte Components Stability and Influence on the SEI Layer Composition

The nature and relative amount of lithium salt and solvent in the electrolyte are crucial for the SEI layer composition, as well as explained for the current density. Indeed, the chemistry of the layer, organic or inorganic, determines its stability, porosity, and thickness.

Lithium salt with fluorinated anion emerged as a key component, able to form a stable, inorganic, LiF-enriched SEI layer, which is in line with previous studies on LIBs.[106,107]

With LiTFSI 2 M in dried THF, under 15 bar N_2, Du et al. have recently reported an outstanding result, i.e., an FE* of 99 ± 2% (even if the isotopic experiments led to a value close to 85%). Even if the NH_3 production rate was slightly low at the beginning of the experiment, at the steady state a yield rate of 92 ± 12 μg h^{-1} cm^{-2} was achieved. It is worth noticing that the area of the nickel wire applied as WE for this result was extremely small (0.15 cm^2).[33] Since the lithium salt is imide-based, the salt degradation could be related to nitrogenated compound formation, leading to NH_3 formation misunderstandings. However, the authors argued that results were confirmed by NMR measurements checking $^{15}NH_3$ from a mixture of $^{15}N_2$ + $^{14}N_2$ in an asserted approximated ratio of 1:2 v:v at 15 bar.[33] With the same salt (i.e., LiTFSI), but at 1 M concentration, the formation of LiF in a stable and porous SEI layer was observed after repetitions of CA alternating with the rest step. This technique was performed in a particular coiled WE cell setup, obtaining an FE ≈ 60% (an isotopic test was carried out for a former study with the same setup, but with a different area). However, in this case, the obtained NH_3 production rate was really low, ≈1 μg h^{-1} cm^{-2}.[108] They suggested a less dendritic and more controlled lithium plating occurrence, thanks to a reduced diffusion rate of Li^+ through the inorganic and compact SEI layer, avoiding the non-desired electrolyte decomposition with the excess of deposited lithium.[108] It should be recalled that sulfur-containing salts could be armful for HOR catalysts in a continuous process with a proton carrier coupled with H_2O splitting.

An experimental comparison of lithium salts with different anions (i.e., BF_4^-, PF_6^-, and ClO_4^-), keeping constant the other system parameters, indicated BF_4^- as the best anion for Li-m E-NRR.[43] Even if the bulk electrolyte conductivity was higher for $LiClO_4$, the FE was doubled with the fluorinated salt, reaching values of 71% ± 3% (isotopically verified in a formed study with the same setup) and the EE of 7.7%. PF_6^- salt registered a FE of ≈ 45% ± 3%. With BF_4^-, air-free X-ray photoelectron spectroscopy (XPS) was carried out on used WE and proved the presence of a LiF layer on the highly porous copper WE deposited on an SS mesh with H_2 bubble template (HBT) method. The system proved to be quite stable after the high current CP for 20 min, reaching –2 V versus Li^+/Li at the WE. With the other tested anions, THF oxidation and electrolyte degradation were observed, since the color visibly darkened and the viscosity of the medium increased.[43]

With $LiBF_4$ 2 M in THF + EtOH 1 vol%, an NH_3 production as high as 153.28 μg h^{-1} cm^{-2} at a commercially relevant current density of 1 A cm^{-2}_{geo} was registered in a single compartment batch cell at 20 bar N_2. The FE was increased to 95 ± 3% at a current density of –0.1 A cm^{-2}_{geo}, in line with the previously discussed correlation of high current density with secondary reactions.[43] Moreover, they observed the formation of NH_3-containing compounds in the SEI layer itself and found NH_3 in the gas phase, easier to be separated.[43] For completeness, with $LiClO_4$ 2 M in a batch cell, a notable NH_3 production rate of 28 ± 4 μg h^{-1} cm^{-2} was reported, but the FE remained around only 15% (formerly checked with isotopic study under different experimental conditions) in combination also with a current density as high as 100 mA cm^{-2}.[21] The formation of the SEI layer was studied in operando via time-resolved neutron reflectometry with an electrolyte based on $LiClO_4$ 0.2 M in THF and EtOH 1 vol%. A double SEI layer was observed during the "potential cycling" protocol, made of carbonaceous-organic molecules and insulating products, such as oxidized Li-THF or Li-EtOH compounds in an inner layer. The thickness of the SEI layer was observed to disappear within 2 h of rest status.[101]

As it is possible to note from these results, the salt concentration is another key factor impacting the SEI layer. Du et al.[33] studied the optimal salt concentration (LiTFSI 1.5 M) to obtain a stable LiF-composed SEI layer onto the nickel WE, leading to the stability of the system for 4 days. They suggested that the salt amount should be a compromise between high ion concentrations, correlated to Li^+ availability for E-NRR and SEI layer at the

Table 3. Parameters and performances of Li-m E-NRR experiments conducted in batch electrolytic cells with EtOH as a proton donor.

References	Pressure [bar]	WE	CE	Reference electrode	Lithium salt	Molarity [M]	Potential [V]	Current density [mA cm^{-2}_{geo}]	EtOH [vol%]	Area [cm^2]	FE [%]	NH_3 production rate [$\mu g\ h^{-1}\ cm^{-2}$]	Isotope labeling (for rigorous NH_3 quantification verification)	Impurities
[62]	50	Fe	Pt	Ag	$LiClO_4$	0.2	n.a.	2	1	1.5	58	≈ 6	no	n.a.
[22]	10	Mo foil	Pt	Pt	$LiClO_4$	0.3	≈ –4	2	0.75	1.8	37	51	yes	n.a.
[22]	20	Mo foil	Pt	Pt	$LiClO_4$	0.3	≈ –4	2	1	1.8	40	58	yes	n.a.
[21]	20	Cu (HBT)	Pt	Pt	$LiClO_4$	2	–4	100	1	0.5 (geo)	15	32	yes	n.a.
[33]	15	Ni wire	Cu	Ag wire	LiTFSI	2	≈ –4	36	1	1.2	90	115	yes	n.a.
[33]	15	Ni wire	Cu	Ag wire	LiTFSI	2	≈ –4	80	1	0.05	100	101	yes	n.a.
[43]	20	Cu (HBT)	Pt	Pt	$LiBF_4$	2	–3 \ –3.5	1	1	0.2 (geo)	73	1500	yes	n.a.
[67]	20	Mo foil	Pt	Pt	$LiClO_4$	1	–4.5	4	1	1.8	56	n.a.	no	O_2 0.8 mol%
[108]	4.5	Cu wire	Cu	Ag wire	$LiCF_3SO_3$	0.2	≈ –4	1.5	1	1.5	56	0.9	no	H_2O ≤0.3 mM
[111]	15	Mo foil	Pt	Pt	$LiClO_4$	0.8	–3.6	2	1	1	28	n.a.	no	H_2O 36 mM
[112]	20	Mo foil	Pt	Pt	$LiClO_4$	0.3	–5	4	1	1.8	79	n.a.	no	O_2 0.8 mol%

WE, and low viscosity of the electrolyte. An increase in viscosity could hinder the mass transport of reactants due to lower ion mobility in the medium.[33]

The solvent itself is a determining factor since its electrochemical stability at the very low E-NRR potential is also correlated to the SEI layer composition, other than to the stability of the process.

The decomposition mechanisms and products obtained have been evaluated for the three more commonly applied solvents in aprotic electrochemical systems, i.e., THF, dimethoxyethane, and diglyme. The process was assessed in a single-compartment batch cell with $LiClO_4$ 0.5 M at a low potential (–3.1 V vs. SHE) and the decomposition products were analyzed with GC-MS. THF has been revealed as the more stable solvent, showing lower concentrations of decomposition products.[109] Even if THF presents the largest potential stability window, further research is needed to find the best option, more stable, with lower vapor pressure, safer, and more sustainable for the process scalability.[110]

Nonetheless, the THF oxidation is the most probable reaction at the anode in these aprotic cells, causing unwanted subproducts presence in the system, higher viscosity due to its polymerization, and introducing irreversibility in this continuous cyclic process. The protons needed for NH_3 formation could be generated from THF instead of EtOH, even if this molecule could be essential to avoid its polymerization.[99]

The oxidation of organic or inorganic pollutants could also be interesting and economically more profitable to obtain the scalability of the process. Moreover, it is necessary to control and avoid the oxidation of NH_4^+ ions, if the product migrates from the WE to the anodic side.[16] For Cherepanov et al., this risk could be excluded because of the low applied voltage window (from –1.5 V to –0.8 V vs. Li^+/Li) in their settings, and due to the EtOH presence that lowers the low anodic pH, contrasting NH_4^+ migration and diffusion to the anode.[108] In another system, NH_3 was found in the anodic compartment even if a membrane was present between anodic and cathodic compartments. Indeed, the applied membranes are commonly proton-selective to allow the H^+ to pass. For example, Lazouski et al. assessed the permeability of a commonly used membrane, i.e., the 175 DARAMIC, which revealed NH_4^+ presence at the anode and an NH_3 loss in the cell after a time of only 40 min.[16]

The impurities in the electrolyte also play a role in the SEI layer formation and in the system stability.

The amount of residual H_2O in the electrolyte is commonly agreed to be detrimental both for electrolyte degradation and for HER predominance over E-NRR.[101,109] A recent study claimed that the optimal amount of H_2O is 35.9 mM, still a very low amount. With an electrolyte made of $LiClO_4$ 0.8 M in THF with EtOH 1 vol%, this amount should allow a more permeable SEI layer thanks to Li_2O addition, bringing to an FE of 27.9 ± 2.5%.[111]

Traces of O_2 have proved to be beneficial for the system.[67,112] The THF solvent degradation products obtained with a variable O_2 content, from 0% and 3%, were characterized with NMR and GC-MS. The optimal amount was concluded to be O_2 0.8 mol% at 20 bar total pressure; this concentration caused a limited number of THF sub-products, the main of which was poly-THF.[67] At the same O_2 concentration, a FE of 78.0 ± 1-3% and an EE of

11.7 ± 0.5% (calculated without considering compression energy) were obtained from "potential cycling" experiments in a single batch cell pressurized at 20 bar, with $LiClO_4$ 0.3 M in THF, EtOH 1.0 vol%, and a molybdenum WE;[112] isotopic tests were carried out for a former study in the same laboratory. At 10 bar, the optimal O_2 amount doubled. Authors suggested, also in these cases, the formation of a more favorable SEI layer, more defective and penetrable. The competition of lithium deposition with the O_2 reduction reaction could lead to delayed Li^+ transport and a more controlled lithium monolayer, keeping an optimal ratio between H^+, N_2, and plated lithium. Moreover, the WE drifting is retarded and the system stabilized.[67]

These findings could also lower the cost of N_2 separation from the air, increasing the competitivity of E-NRR process with respect to the HB one.

Since, as discussed, all elements contribute to the SEI layer composition and affect the process performance, for each modification of a single factor the optimal amount of the other parameter could be modified.[93]

4.6. Li-m E-NRR in Aprotic Electrolytic Systems: Final Comparison

As described above, each element of the system influences the complete E-NRR process. **Table 3** lists the THF-based experiments discussed in the previous sections, and some correlations are extrapolated from a direct comparison of experiments in batch cells and with EtOH as the proton donor, i.e., a setup in which the majority of electrolytes have been screened toward the achievement of higher FE and NH_3 production rate. From these findings, the verification of the optimal components and amount should be assessed every time the setup is changed. In particular, the EtOH optimal amount is different in the emerging flow cell system with GDE and the proton carrier, able to guarantee a more stable process and couplable with the H_2O splitting and the HOR at the anode.[69]

The influence of proton donor amount and lithium salt concentration in the electrolyte on the overall performance is illustrated in **Figure 6**a,b, where the area corresponds to each specific figure of merit value, as in the title of the graph (FE on the left, NH_3 production rate on the right).

Even if a clear trend of the figures of merit is not evident, it is possible to observe that higher performances have been mainly achieved with a higher molarity of lithium salt in the electrolyte (i.e., 2 M), particularly if the salt presents a fluorinated anion. As discussed previously, this element, if well equilibrated with the EtOH amount, could ensure higher stability thanks to the LiF-containing SEI layer, able to control the protonation rate.

Other interesting observations are coming from the performance dependence on electrochemical fundamental parameters, such as the electric current density and the applied potential, plotted in Figure 6c,d. It is possible to distinguish a clear classification in two main groups, i.e., the $LiClO_4$ salt systems and the fluorinated salt ones. The plot again highlights that better results can be achieved using fluorine-based compounds. The application of these salts stabilizes the process and allows higher current density to be applied, opening up the opportunity of scaling up the process. When fluorinated salts were used, the NH_3 production rate obtained at high current densities showed an opposite trend in comparison with the FE. As previously discussed, the application of higher currents favors secondary reactions, thus lowering the FE.

In the electrolytic aprotic systems, some factors not yet discussed in this review should be deepened, such as the electrode chemistry. The reference electrode itself is quite a big deal in organic electrolytes since it is not possible to establish a universal scale of potentials like it has been done for RHE, due to changes in solvents or salts, which vary the measured potential. Platinum stability in the system is also still uncertain. A few groups are raising concerns on these aspects and should be deepened in the future to avoid misunderstandings. An electrode made of $LiFePO_4$ has been proposed as a more stable reference.[113,114] The CE should not participate in the reaction, being inert; for example, if iridium is used, NH_3 oxidation has to be considered as well (see Section 4.5.3). Different metals have been studied as WE, but the variation of the FE observed due to this factor was inferior to that obtained from the previously listed factors' variation. In this Li-m strategy, the WE material is supposed to be inert, guaranteeing the highest specific surface area possible to make E-NRR happen on plated lithium.

For this reason, the addition of a catalyst is also rarely considered. A material able to accelerate electron charge transfer at the interface could improve the kinetics and overall performance. As a matter of fact, previous results highlight the reduction of the gap between the E-NRR and lithium deposition kinetics as a main issue in this system. However, at the current stage of the research, the evaluation of other catalysts in combination with this mediator would just add complication to a system not yet explored enough, and for now this is not the main focus, but it could be probably developed as a future implementation of the system. A gold catalyst over a carbon paper support with $LiClO_4$ 0.2 M in THF was observed to reduce the E-NRR overpotential from –1.75 to –1.08 V versus Li^+/Li, in contrast to what happens in aqueous systems;[20] those results were also confirmed by DFT calculations of the adsorption energy. Besides, authors employed in situ XRD to study the Li_3N amount on the cathodic surface, and they observed how it notably increased, while lithium intercalation on the carbonaceous support was avoided, and blocked by the surface layer. This unnecessary electrochemical reaction would decrease the FE, which was registered as high as 34.0% and with an NH_3 yield of 50 μg h^{-1} cm^{-2}.[52]

The growing argumentation in the literature on the reaction mechanism and on the effectively active species at the interface highlights that a key matter to be addressed at this point of the research is how the potential/current application (and what value) is beneficial to increase FE, EE, and production rate, without mining the stability of the whole system. Indeed, if the current would not be addressed entirely to lithium plating or to N_2 reduction (in the case this undergoes a chemical reaction), it could be related to the unwanted degradation reaction of the electrolyte and formation/decomposition on the SEI layer. An increase of the current density toward a scale-up system (as mentioned, industrialization requires at least 10 mA cm^{-2}) could bring with it uncertainty on system optimization.[91]

In conclusion, even if many variables have been changed between different studies, such as the architecture itself, and it is

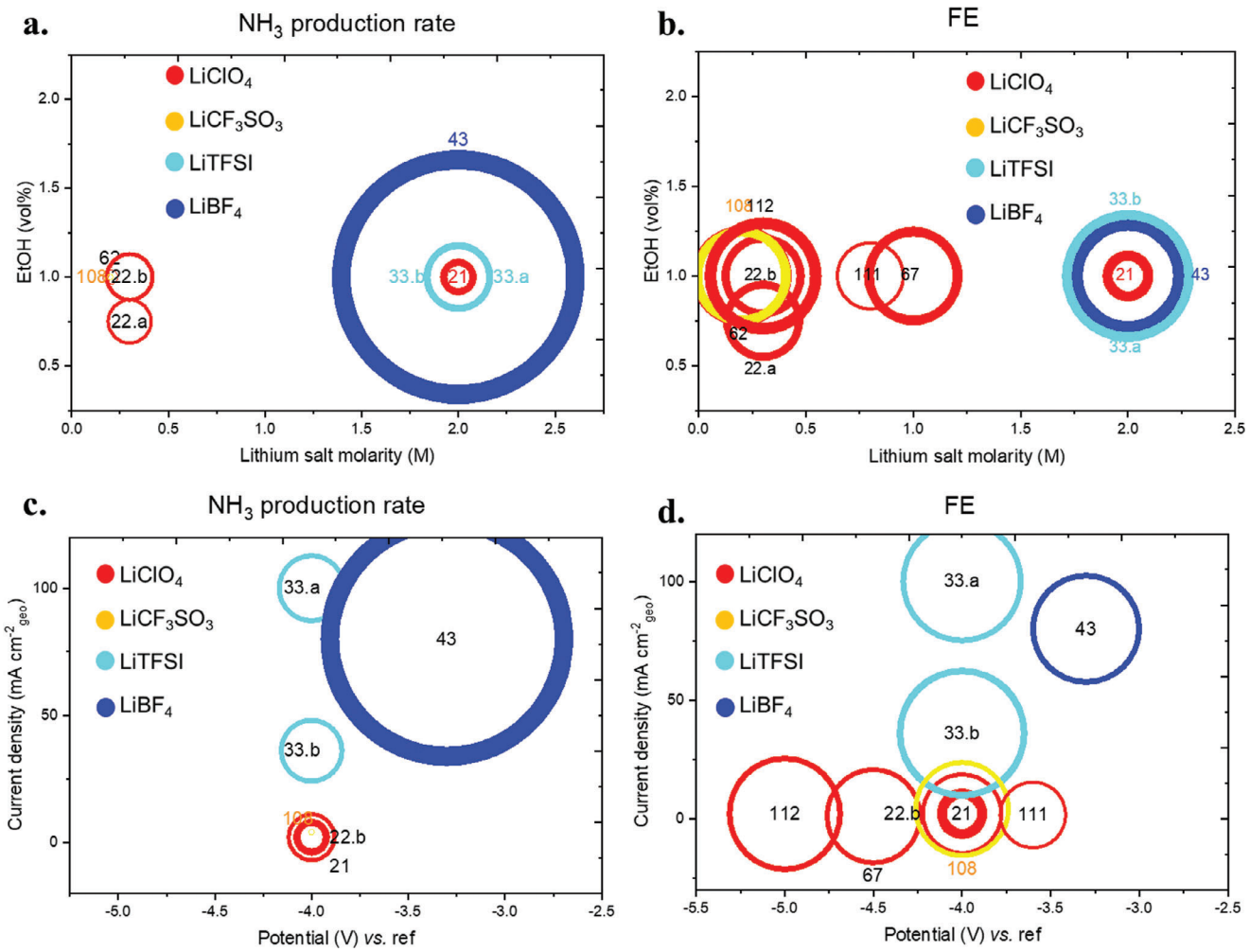

Figure 6. Effect of lithium salt type and molarity, as well as of EtOH concentration in the electrolyte, on the a) NH_3 production rate and b) FE of the process. Effect of applied potential and current density on the c) NH_3 production rate and d) FE of the process. The area of each circle is proportioned to the specific value of each figure of merit. The numbers indicated in each circle correspond to the bibliographic references.

not possible to observe a clear trend or to precisely select a single parameter or condition able to drastically increase the performance, there are some factors that emerged as the most influent parameters:

- SEI layer composition: its stability under high current or voltage could be mainly determined by the fluorinated anions and EtOH presence, which are able to form a quite stable layer, but still penetrable from N2 and protons, also controlling the Li+ plating on the WE.
- Lithium plating protocol in correlation to the SEI layer stability: the relative ratio of reactants, in combination with the potential application (or current) driving force, determines the selectivity toward the E-NRR and NH3 production.

Indeed, excluding structural factors, i.e., the reactor type (correlated to N_2 pressure influence and availability in the cell) and the geometric surface areas (that mathematically influence the yield), the electrolyte formulation emerged as the highly impactful factor on the stability and durability of the process. To engineer the SEI layer in a tailored deposit with specific characteristics, i.e., both stability and reactants ratio regulation, the chemistry and degradation mechanism of the electrolyte species in the cell should be deepened. The wide literature available from LIBs and LMBs could be taken as an inspiration.[95] Even if fluorine presence in the SEI layer led to its increased mechanical and chemical stability (as in LIBs), N_2 affinity as well as Li^+ and H^+ diffusion restrains appeared more dependent on the organic-oxidized components.[99] In future studies, the design of a bifunction layer obtained from the decomposition of both the salt anion and a proper proton donor/shuttle should be further investigated in dedicated studies. Results obtained from different combinations of relative amounts or subsequent additions of electrolyte components seem to hide correlations between these variables: this research could be fastened by the application of the statistical method of the design of experiment (DOE). This method is a powerful tool to plan an experimental campaign that, with a restricted number of experiments in comparison with one-factor-at-time, allows to prediction of the behavior of a system under the variation of established factors. Moreover, the results could be

statistically analyzed to gain an understanding of process trends and system optimization.[115]

4.7. Molten Lithium Salt Systems

In the molten lithium salt strategy for Li-m NH_3 production, the N_2 gas flows into a bath containing different molten salts and, with the simultaneous addition of H_2 or H_2O vapor, NH_3 is formed and recovered as the main gas emitted from the reactor.[116] The spontaneous separation of NH_3 from the solution drives the equilibrium toward NH_3 production. These techniques could be applied for chemical or electrochemical N_2 reduction processes at ≈ 400 °C but at a lower pressure than that used for the HB process. Nevertheless, the poor ionic conductivity of the solvent has been found to limit the kinetics of this pathway.[117]

The co-presence of lithium, H^+, and N_2 could generate different intermediates, depending on process conditions. LiH, one of these possible intermediates, is often claimed as an unwanted but unavoidable sub-product of the molten salt methods since its formation is favored above 100 °C. However, it is also considered a strong reducing agent able to assist N_2 fixation.[118] The reaction of LiH with N_2 has been experimented with via the "chemical looping" of two semi-reaction steps, demonstrated with MS and XRD analysis,[119] as reported below:

$$4LiH + N_2 \rightarrow 2Li_2NH + H_2 \quad (8)$$

$$2Li_2NH + 4H_2 \rightarrow 2NH_3 + 4LiH \quad (9)$$

Lithium imide (Li_2NH) product presents a favorable pathway since it quickly splits into LiH and NH_3, even at 250–300 °C.[120]

Even in a liquid phase, lithium behavior appeared unique in comparison with other alkali metals. Li_2NH behavior has been predicted thanks to an innovative modeling method developed by Parrinello's research group, which combines DFT with machine learning to evaluate the dynamic of the reaction on a much larger scale and for a wider time scale than DFT studies: at 700 K, the crystal was hypothesized to be in a superionic condition, in which the Li^+ inside the crystalline structure are able to rapidly diffuse between different vacancies, like in a liquid, maintaining the same charge order and the minimum of potential energy.[121] The incoming molecules, such as N_2, are rapidly able to destabilize the Li_2NH surface, entering a "fluctuating", but stable intermediate state. Indeed, this melt can stabilize a labile intermediate such as Li_3N in the reaction medium. On the other hand, the hydrogenation step may deteriorate the melt, forming LiH and depleting the mediator and, under specific conditions, may lead to the re-formation of Li_2NH or $LiNH_2$.[118] However, the main irreversibility has been suggested to be the agglomeration of the intermediate products of Li_2NH particles, which leads to a cascade effect with sluggish kinetics, slower H_2 diffusion, and a plateau of the figures of merit.[119] The addition of ball-milled cobalt particles allowed a longer cyclability and durability of the system.[118]

Molten lithium was also tested in alloys: the ability of tin and group-14 metals (e.g., silicon, germanium) to maintain lithium dissociation properties toward N_2 was investigated by DSC and XRD.[122,123] Lithium is supposed to dissociate N_2 in a more controlled way thanks to the stabilization by the transition metal. This phenomenon of a chemical shift called the Knight's shift, should reduce the nuclear magnetic resonance of lithium (in similarity with intercalated lithium),[124] maintaining lithium's high mobility. Li_7Sn_2 has been proven as reversible during NH_3 production.[125]

This strategy was tested in an E-NRR process in combination with an alkali-metal halide melt.[126] Lithium molten salt mixture of the alkali-metal halides LiCl/KCl and LiCl/KCl/CsCl was tested in 2002 by Murakami et al. [116,117] N_2 was fluxed into the melt, reduced on nickel cathode into N_3^-, which was stabilized at ambient pressure by LiCl, then easily hydrogenated in imide NH^{2-}, amide NH_2^-, and then NH_3 by the addition of H_2. Gaseous NH_3 was released from the melt at 400 °C. The FE measured by GC-MS analysis was quite remarkable, as high as 73% at a cathodic potential of 0.4 V versus Li^+/Li, but Li_3N 0.2% mol of was added to the melt in order to favor N_2 reduction into N^{3-} and could lead to NH_3 production. NH_4Cl was also formed but was hard to separate.[116,117] These studies are considered to be oversimplified by Mcpherson et al.[24] They tested again the same system and obtained an exaggerated FE (higher than 100%) and NH_3 yield, even without further N_2 flow or current in the cell. With LiH as the initializing agent instead of Li_3N, the FE* was only 5%. Moreover, the intermediate products, such as Li_2NH and $LiNH_2$ were accumulated in the melt and could lead to instability in the cell, causing an anodic-cathodic "inversion" of the potential.[117]

Tang et al. tested a bi-phase system at ambient pressure with two immiscible solutions, combining lithium alloying and halides strategy. The lighter solution was molten LiCl/KCl, in which H_2 is bubbled and gaseous NH_3 is produced, thanks to Li_3N, coming from the lithium-tin liquid alloy set below. Indeed, in the solution below, Li_3N was continuously produced due to the reaction of N_2 gas bubbling and the LiH residue, sinking from the above melt as a byproduct and converted at the alloy-salt interface of the two solutions by tin alloying.[126] The process was stable for 81 h with an average NH_3 yield rate of 90 μg h^{-1}. However, the process required ≈ 500 °C and pure flow of H_2 and N_2, since O_2 and H_2O impurities could slow down and create irreversible products such as Li_2O.[126]

The melting strategy is also evaluated for other aspects of the whole E-NRR process, thanks to the not-so-high lithium melting temperature and the higher mobility of lithium in this phase. The third step (Li^+ recovery with subsequent lithium metal replenishment) could be done in electrochemical reactors with LiCl/KCl molten salts, as nowadays they are applied for industrial lithium metal production via LiCl electrolysis at 3.6 V versus SHE at 427 °C.[17]

Sodium or potassium hydroxides have also been considered as molten media for E-NRR. A process efficiency of 35% was obtained from air and steam at 200 °C and ambient pressure, thanks to the electrolysis process in a molten solution of NaOH and KOH 1:1 with nano-Fe_2O_3 particles, while a current density of 2 mA cm^{-2} with 10 cm^2 electrodes was achieved. This solution presented a eutectic composition, which allowed the temperature needed for the formation of the melt to be lowered;[127] however, the publication was then retracted since NO_x^- traces were present in the Fe_2O_3 particles.[128]

In conclusion, since 1977 the use of a mixture of different nitrogen-containing lithium salts has been studied, and the formation of Li_3N and NH_3 was proved.[129] However, the high

temperature needed, in combination with the low selectivity registered toward NH_3, implies that this strategy leads to massive consumption of lithium-containing species in secondary products. Indeed, recently the molten salts appear not appealing as the promising results in Li-m E-NRR strategy in organic solvents. The equilibrium should be better understood to find the best temperature and process conditions to move the reactions toward N_2 fixation.[130,131,132] Moreover, the profitability of using an azo compound for NH_3 production is arguable. Different $Li_xN_yH_z$ compounds formed in the lithium salt baths as Li_2NH are nowadays more often evaluated as an H_2 carrier solution.[133,134] The study of reactions of $Li_xN_yH_z$ compounds could be interesting in the Li-m E-NRR field to better understand the intermediates and the phenomena of the N_2 fixation with lithium in the presence of protons, as well as the reactivity of amides of other alkali metals, e.g. KNH_2 and $Ba(NH_2)_2$.[135]

5. Stepwise Processes

In this section, the discontinuous processes are illustrated. "Stepwise" indicates that the three reaction steps listed in Equations 4–6 (i.e., lithium reduction, nitridation, and Li_3N hydrolyzation in NH_3) are conducted in a different environment and/or time. The whole process is inevitably discontinuous, since the reaction conditions change in each step, in order to maximize the selectivity toward the product of interest of each step (e.g., Li_3N, NH_3, and metallic lithium). They are subdivided according to the nitridation step reaction type, whatever thermochemical or electrochemical Li_3N formation. In the case of the thermochemical lithium nitridation processes, the rate-limiting step is the thermochemical direct reaction between lithium and N_2. Li_3N could be formed electrochemically in Galvanic Li—N_2 cells, an interesting device recently proposed in the energy storage field, that opens promising possibilities to enhance the kinetics, energy efficiency, and selectivity of the nitridation step.[136] Some examples are reported and compared in the following sections.

The main advantage of the stepwise pathways is that Li_3N is hydrolyzed with H_2O in a second step, without the need for an organic proton donor to be consumed, neither H_2O splitting + HOR integration. The energetic and economic benefits of direct H_2O protonation are detailed in **Section 6**.

After Li_3N hydrolyzation, LiOH is the residual by-product, from which lithium recovery is mandatory and it represents the most energy-requiring step. Anyway, it is possible to electrify this process using an electrochemical cell to reduce Li^+ into metallic lithium, closing the cycle.

5.1. Direct Lithium Nitridation

The thermochemical direct reaction of lithium with N_2 gas flow avoids problems of N_2 mass transport limitation in an electrolyte medium, as well as circumvents selectivity issues. Indeed, none HER, nor electrochemical degradation reactions limit the FE, and Li_3N is spontaneously and exothermically formed in a controlled reactor even under mild conditions.[17,59] However, the nitridation of lithium bulk is sensibly decelerated (**Section 3**) and, even if the production rate could be boosted at high temperatures or pressure, the utilization of the alkali metal could result incomplete.[64] Anyway, the use of copper particles rolled with metallic lithium showed impressive quick Li_3N formation in the direct nitridation process in a study by Zang et al.[137] Similarly to the HB one, this step needs pure N_2 gas as the feed, to avoid the formation of a thick passivation layer on lithium surface by impurities or Li_3N conversion in unwanted species. Impurities will drastically slow down the reaction and decrease the EE, as observed by differential scanning calorimetry (DSC) and XRD analysis.[26]

Since lithium utilization is not optimized by this strategy, many studies on direct thermochemical nitridation evaluated also the step of Li^+ reduction into lithium metal in an electrochemical cell. The electric current, in this scenario, is applied with the aim of lithium recovery, and the FE should be calculated for the whole process.[138,139,140] Experimental tests focused on the passage of Li^+ from an aqueous solution to an aprotic environment, where Li^+ is reduced into a metallic layer. Due to the exceptional reduction potential of Li^+, this electrolysis has to be protected from H_2O by an aprotic environment.

To achieve this condition, and take inspiration from the LMB-air field, the use of a glass ceramic membrane called LISICON, selective for Li^+, was proposed by Kim et al.[138] They used a two-compartment electrolytic cell with H_2O and polycarbonate (PC) electrolytes, containing Li_2SO_4 1 M and $LiClO_4$ 1 M, respectively. The whole process for NH_3 production presents three steps: i) lithium plating is studied on a nickel cathode; ii) lithium nitridation takes place at 220 °C for a maximum of 2 h; iii) Li_3N protonation is performed in H_2SO_4. This compound allows $(NH_4)_2SO_4$ to be directly obtained as the product. Li^+ remaining in the aqueous chamber of the electrochemical cell is then applied in the third step and deposited as lithium metal in the aprotic chamber, closing the cycle, with a final FE of 52.3%.[138] The SEI layer formation onto deposited lithium was observed as the main limiting factor for the FE of the system. To overcome this problem, the use of $CsClO_4$ as an additive for the PC electrolyte was assessed. Lithium deposition presented in this case a more regular structure and the unstable and thick SEI layer rich in lithium-organic compounds was avoided.[139] Since the LISICON membrane presents problems of high cost and scarce durability, an alternative membrane-free approach was also investigated, exploiting the properties of the immiscibility of H_2O and PC. Such a separation resulted even more enhanced thanks to the addition of 1 wt% of highly hydrophobic poly(methyl methacrylate) in the PC electrolyte, partially avoiding Li^+ losses in H_2O and unwanted LiOH formation in the system. In this case, the overall FE* raised to 57.2% and the production rate reached 0.74 μg h^{-1} cm^{-2}.[140] Li^+ could also be recovered with the use of solid selective polymeric electrolytes, as already proposed by some groups active in lithium recycling projects.[141]

A particular and intriguing process is the stepwise solution based on N_2 and H_2O proposed by McEaney et al.[17] The lithium recovery was operated by the LiOH electrolysis in a molten lithium salt proton-free environment, followed by direct lithium nitridation and Li_3N hydrolyzation into NH_3. The whole process took place in a three-area rotation reactor, as shown in **Figure 7a**.[17] This lithium cycling strategy is closed with NH_3 and H_2O separation from residual LiOH through evaporation at 120 °C. An initial FE of 88.5% was achieved from the whole process, confirmed with an isotopically labeled test.

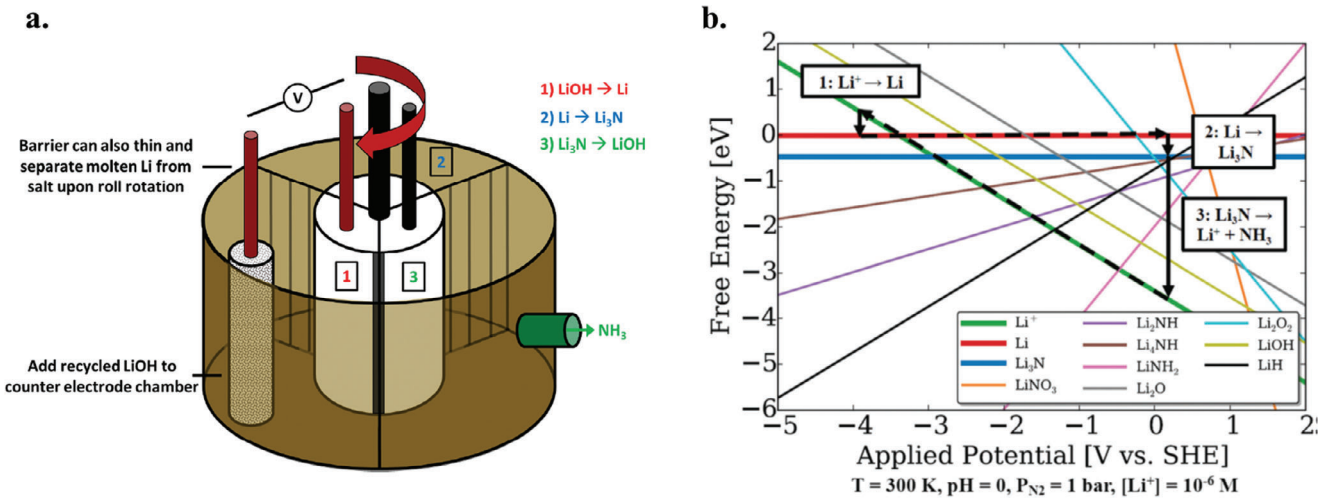

Figure 7. a) Conceptual design of the stepwise cyclic device proposed by McEaney et al.[17] The roll in the middle acts as a segmented working electrode: in step one, molten lithium, refurnished by LiOH insertion, is plated on the roll. The plated lithium is then exposed to N_2 gas thanks to the roll rotation and a thin film of Li_3N is obtained in step 2. The rotation of the roll in the third section, where H_2O is added, gives hydrolysis into NH_3 production. Finally, the same roll surface returned to step 1 as a fresh electrode surface to continue the cycle) b) Phase diagram obtained at 300 K, pH 0, and a Li^+ ion concentration of 10^{-6} M. The diagram shows the relative thermodynamic behavior of lithium, nitrogen, oxygen, and hydrogen species with the proposed lithium cycle steps superimposed) Adapted and reprinted with permission from.[17]

To evaluate the process parameters, a phase diagram, reported in Figure 7b, was obtained at 300 K, pH 0, and a Li^+ ion concentration of 10^{-6} M. The diagram illustrates the selectivity dependence on the system variables. They defined the proton donors as "thermodynamic sinks" for lithium reduction due to their predominant activity to HER and sub-products with lithium. Indeed, they suggest operating lithium reduction in the absence of protons to critically enhance the selectivity toward NH_3.

They applied an electrochemical cell for lithium recovery with a molten salt solution as electrolyte, similar to molten salt baths for NH_3 continuous production (**Section 4.7**): a molten salt mixture of LiCl/KCl at the cathodic compartment and LiOH/LiCl at the anodic one. Recovered Li^+ migrated from the anode to the cathode. At the anode, O_2 and H_2O evolved. To ensure isolation and prevent unwanted or reverse reactions of the alkali metal, a porous alumina layer was placed between the two compartments. They set a temperature of 450 °C and a cell potential of –3.3 V versus SHE or lower, not very far from the thermodynamic one (i.e., –2.8 V vs. SHE at 427 °C).[17]

They calculated the efficiency of lithium recovery as high as 98% and a lithium-plated layer of 1 mm thick was obtained, from which a near complete nitridation occurred after only 12 h at 22 °C. This strategy, even if not anymore considered in recent papers, suggests how the simplification of the system could reach easily competitivity with the HB counterpart avoiding protons and organic solvent degradations during the lithium nitridation step.

The mentioned technology for Li^+ recovery and reduction can be applied also for a stepwise process in which the nitridation step is operated in Li—N_2 Galvanic cell for Li_3N production. After the cathode, where nitrogen-containing species are accumulated, is protonated, the sub-product obtained from the cathode washing, containing both NH_3 and LiOH, can be treated as in the detailed strategy of this Section.

5.2. Li—N_2 Cells for Li_3N and NH_3 Production

Stimulated by the increasing attentiveness to metal-gas batteries, research groups are now starting to turn their attention toward Li—N_2 devices. Deepening knowledge about the electrochemical reaction between lithium and N_2 in a completely aprotic environment could open, indeed, new possibilities both for energy storage and NH_3 production.[25,142]

With Li—N_2 cells, the Li-m E-NRR process has to be rethought from scratch. Indeed, in this case, it is no longer an electrolytic cell, but it is a Galvanic cell: the electric energy should be produced from lithium oxidation into ions at the anode and the simultaneous desired N_2 reduction into Li_3N. Li^+ migrate from the anode to the cathode, where they arrive in contact with N_2, fed as gas through the GDE, and Li_3N is accumulated on the cathode surface. This reaction is spontaneous and the chemical energy conversion into electric energy during the discharge of the cell could be further exploited. The next step is the protonation of the intermediate product (i.e., Li_3N) accumulated on the cathode, fluxing H_2O (or H_2O vapor) in the system, or moving the cathode in a second reactor for batch hydrolyzation. Then, LiOH has to be recirculated, as described in Section 5.1, closing the cycle.

The reaction between lithium and N_2 in the electrochemical device has been under study for several years in the energy storage field, especially that of Li-air batteries. Theoretical calculations suggested that Li—N_2 batteries could reach an energy density comparable to that of rechargeable Li-SO_2 and Li-CO_2 batteries, as high as 1248 Wh kg^{-1}, even if lower than Li-air (i.e., Li—O_2) counterparts.[28] However, to obtain the theoretical capacity and apply this technology in the energy storage field, it is necessary that the Li_3N product is reversible. This issue represents a crucial drawback for Li—N_2 batteries, but for the E-NRR it is not necessary, since the obtained Li_3N is then recovered and/or hydrolyzed into NH_3.

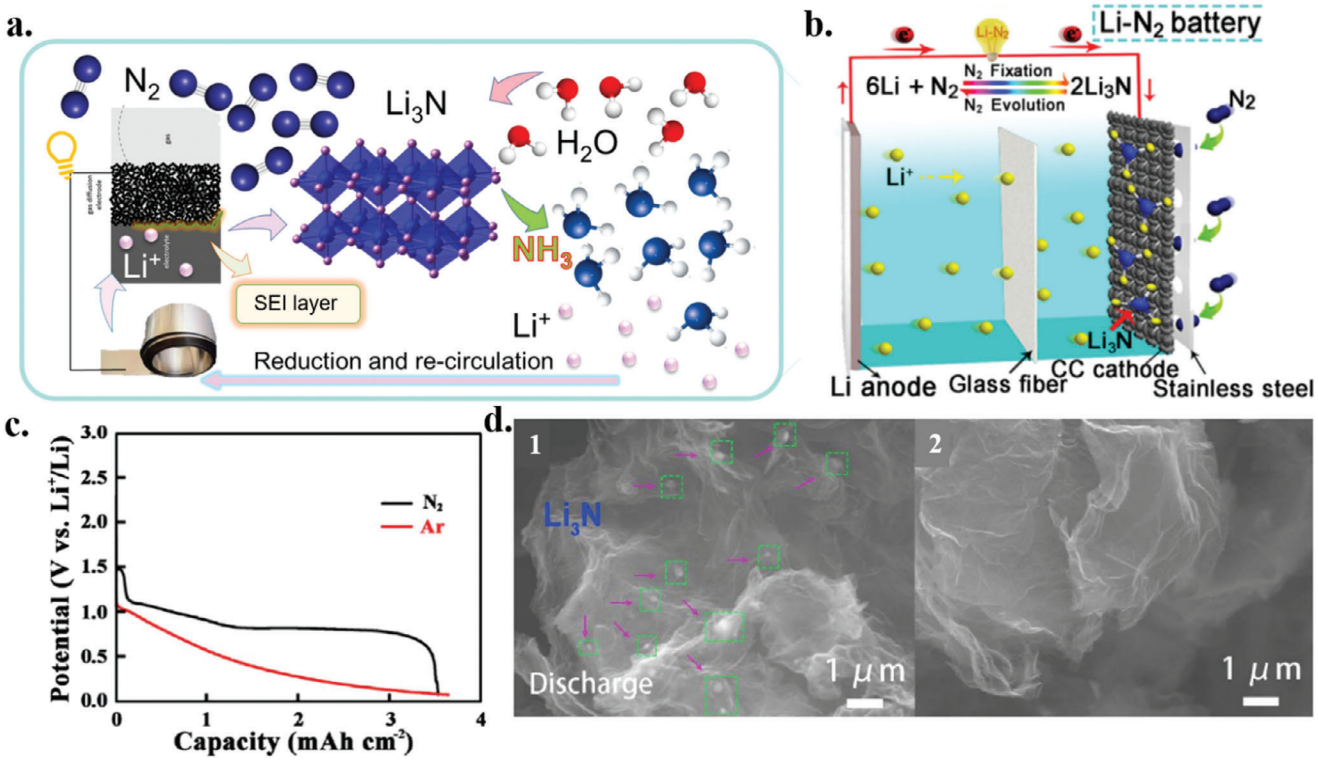

Figure 8. a) Li—N_2 schematic cell structure) On the left, a) representation of the cell components: metallic lithium is oxidized into Li^+, which migrates to the cathode, where the porous carbonaceous layer of the GDE reacts with electrons and N_2 gas, forming Li_3N, which is then hydrolyzed into NH_3. Li^+ are released, reduced, and re-circulated into a new anode for the cell. b) The cell architecture adopted by Ma et al. Adapted and reprinted with permission from.[28] c) Galvanostatic discharge profile of Li-gas cells composed of a lithium metal anode, a glass fiber separator with $LiCF_3SO_3$ 1 M in TEGDME, and a carbon cloth GDE cathode) Scan rate applied of 0.05 mA cm^{-2} and cutoff potential of 0.08 V versus Li^+/Li. The red curve corresponds to the test performed fluxing argon inside the cell, while the black one is in the presence of N_2 flow in the saturated cell. Under N_2, an additional plateau was registered at ≈ 1 V versus Li^+/Li. Adapted and reprinted with permission from.[28] d) SEM micrographs of tested nitrogen-doped carbon added with Mo_2C nanoparticles: 1) The cathode after the galvanostatic discharge in a Li—N_2 cell with $LiCF_3SO_3$ 1 M in TEGDME, until 0.8 V versus Li^+/Li, at a current density of 50 mA g^{-1}, with a cutoff capacity of 0.5 mAh; 2) The small particles deposited disappeared after the galvanostatic charge at the same conditions until 4.5 V versus Li^+/Li, suggesting Li_3N formation and reversibility. Adapted and reprinted with permission from.[145]

In a Li—N_2 cell, the direct reaction between N_2 and lithium anode should be prevented: as for Li—O_2 batteries, the gas cross-over through the separator could be a detrimental factor and would result in misunderstandings in the NH_3 production field.[143] Indeed, the metallic lithium at the anode may spontaneously form Li_3N and this uncontrolled product could lead to misunderstandings, in particular, if any proton donor is present and would be able to form NH_3 reacting with anodic Li_3N. Even if the technology is in its infancy, this stepwise electrochemical controlled system is promising to achieve high stability, long-lasting, and efficient NH_3 synthesis from N_2 and H_2O.[25,28,144]

5.2.1. Li—N_2 Cells: Architectures and Reactions

In 2017, Ma et al. were the first to investigate a Li—N_2 system and demonstrated a proof of concept of a rechargeable cell forming Li_3N at the cathode at ambient temperature and pressure.[28] N_2 fixation in the cell was performed with a CA of 5 h at 1.08 V versus Li^+/Li, a potential higher than that of lithium plating. Authors claimed a FE of 64% and 81%, respectively, without and with the addition of ruthenium nanoparticles as catalyst on the carbon paper GDE.[28] At that time, the isotopic labeling experiment was not yet commonly carried out to confirm the results. **Figure** 8a,b shows a schematic representation of this device.

As architecture, they adopted a commercial in-flow cell from EL-Cell GmbH designed for testing Li-gas batteries; it is a one-compartment SS cell with a gas inlet for GDE cathodes on the top and a closed bottom for metallic lithium anode. The electrolyte, spread on the fiberglass separator, was $LiCF_3SO_3$ 1 M in tetraethyleneglycoldimethylether (TEGDME). TEGDME was previously studied for other Li-gas batteries due to its low volatility and high ionic conductivity, as well as relative stability to lithium metal. However, it presents some safety issues concerning fertility, and several groups are working to replace it.[143] The carbon cloth was applied as GDE, chosen as a good compromise between a conductive network and a high surface support for catalysts and products developed in a three-phase system (see Section 5.2.4 for details on GDE characteristics required for this cell architecture).[28] The plateau in the discharge potential profile (Figure 8c) suggested a reaction with N_2 at ≈ 1 V versus Li^+/Li. To investigate the electrochemical reaction between N_2 and Li^+, CV tests were performed at a very low scan rate (0.05 mV s^{-1}) under

argon or N_2 flow; an additional peak was registered only in the presence of N_2, while a more intense peak registered with both gasses was referred to the unavoidable intercalation reaction of Li^+ into the graphitic cathode.[28] This last phenomenon is supported by a shift in the XRD pattern, referable to a distancing of graphite crystalline planes.[25] Li_3N production was supported by the XRD pattern, FTIR spectra, and SEM analysis of the cycled cathode. SEM images showed dispersed particles that vanished after the charge step, suggesting the reversibility of Li_3N. EDX spectrometry elemental mappings showed a uniform distribution of nitrogen on the cathodic surface.[28]

Therefore, the process inside the cell was formulated as follows:

$$6Li + N_2 \rightleftarrows 2Li_3N \quad (10)$$

Despite this promising proof of concept, some issues were pointed out for this technology: the anode is unstable due to both the dendrite growth during lithium plating/stripping, a well-known issue in LMBs,[146,147] and due to the N_2 gas cross-over through the separator. The decomposition of the electrolyte at the cathode interface is even in this system a crucial factor, covering with the SEI layer the active sites, as observed with XPS analysis. The potential window applied is wider than that in LMBs and the electrolyte formulation should be optimized for this system, even if the potential applied is higher than in the electrolytic cell of **Section 4**.

The study by Wang et al. proposed a similar Li—N_2 system as a storage device with N-doped carbon added with Mo_2C nanoparticles as the cathode.[145] Mo_2C has been widely tested as a catalyst for E-NRR, its activity was confirmed also by the DFT study.[148] For the cathodic carbonaceous support, the nitrogen-doped carbon proved good electrical conductivity, with a favorable morphology with both macro-channels and mesopores, suitable for storage of high amounts of the desired discharge product, i.e., Li_3N.[149] The presence of nitrogen atoms in the cathodic material could increase misunderstanding for the NH_3 production; the product quantification was not even assessed in this case, since the main focus of that work remained the effective Li_3N reversibility. N_2 reduction was suggested by the CV from an additional reduction peak at ≈ 1.5 V versus Li^+/Li, absent in argon-saturated cells. They supported the presence of Li_3N particles[145] with SEM (Figure 8d) and EDX analysis. However, the intensity of the peaks referred to Li_3N was weakly recognizable by XRD, in comparison with the instrument noise.[145]

The reversibility of Li—N_2 battery has been analyzed in-depth by Zhang et al., with the main focus on the application as an energy-storage system.[25] Tests were performed in a glove box filled with high-purity N_2 on an open coin cell setup. The cathode, made of graphene nanosheets, was coupled with $LiClO_4$ 1 M in TEGDME. The formation and decomposition of nitrogen-containing compounds during discharge and charge, respectively, were verified with EDX, XPS, and SEM analyses: nanometric agglomeration and dissolution of particles present at the cathode were confirmed but with a very low relative increase (of ≈ 1% on the atomic amount of nitrogen). Li_3N presence was further verified indirectly, thanks to the measurement of NH_3 obtained from its protonation, by a portable NH_3-analyzer: during the first discharge, an NH_3 amount of 0.37 ppm was measured, increased at 0.74 ppm after the 5th discharge.[25] The presence of NH_4^+ was assessed by ^{1}H NMR after 50 h of discharge at 100 mAh g^{-1}, coherently with the NR colorimetric test. ^{1}H NMR spectra and XRD pattern revealed the presence of another main product, i.e., LiOH. The unwanted degradation of Li_3N with the traces of H_2O and O_2 was suggested as follows:

$$Li + N_2 + H_2O \rightarrow LiOH + \text{nitrogen containing compounds} \quad (11)$$

$$Li + N_2 + \text{oxygen containing substance} \rightarrow Li_xN_yO_z \quad (12)$$

The metallic lithium anode was also studied; lithium was exposed to the glove box atmosphere filled with N_2, and the spontaneous Li_3N formation rate was studied along with its stability. SEM analysis at different times showed that the lithium surface became more and more porous. Li_3N was observed on the lithium surface, but then it was found to be spontaneously covered by LiOH, as confirmed by XPS. The detection of lithium/nitrogen/oxygen compounds on the surface confirmed that the Li_3N formed at the cathode could, upon time, be spontaneously converted by impurities.[25]

Lithium surface was studied after cycling: SEM analyses revealed a flat and smooth surface, with large crevices filled with both Li_3N and LiOH, after only 10 cycles. This inorganic passivation layer on the anode was observed to be beneficial and able to suppress dendrite growth. Moreover, the carbon corrosion promoted by the cell polarization was speculated, as similar to what occurs in Li—O_2 batteries (more detail in Section 5.2.4). At the cathode, the formation of Li_2CO_3 was observed in the SEI layer, resulting in poor cyclability and efficiencies.[25] In conclusion, this work suggested that Li—N_2 batteries could be rechargeable rather than reversible due to the formation of by-products consisting of lithium/nitrogen/oxygen compounds and LiOH, Li_2O, and Li_2CO_3. Despite these being crucial limiting factors for Li—N_2 as storage devices, the concept of a Li—N_2 cell for NH_3 synthesis could still be interesting. The reversibility is not fundamental for E-NRR: in this scenario, Li_3N has to be protonated, but the setup should be optimized toward this different aim, and specific studies are encouraged.[25]

5.2.2. Catalysts for Li—N_2 Cells

The kinetics of Li_3N formation could be a limiting factor for E-NRR, together with Li_3N instability. Li_3N accumulation at the cathode was supposed to slow down the kinetics, increase overpotential, and block redox species at the cathode.[158] To solve these issues and increase the production rate, different catalysts have been proposed, such as two-dimensional metal-embedded polyphthalocyanines (MPPcs).[150] MPPcs were tested with a computational screening of the E-NRR interaction on two-dimensional metal-organic framework structures composed of macrocyclic ligand framework (able to provide stability to the adsorbed reactant) and different metal centers with tunable oxidation states (scandium, titanium, vanadium, manganese, iron, yttrium, zirconium, niobium, molybdenum, ruthenium).[150] Some of the studied metal centers have been already tested toward NH_3 formation (e.g., molybdenum,[151] iron,[152] and a combination of ironmolybdenum),[153] but in this case, the study focused on Li_3N

formation for Li—N_2 battery. The simulation results showed different absorption and reaction mechanisms on the metal centers. For example, iron, titanium, and scandium presented promising low charge and discharge overpotential (close to zero), but still negative adsorption-free energy.[150] Ti_2C was theoretically validated for Li—N_2 batteries.[154]

Highly available and low-cost SnO_2 particles have already been studied for LIBs, supercapacitors, and Li—O_2 batteries,[155,156] has been proposed in combination with iron and enriched with O_2 vacancies for N_2 absorption and activation.[157] The discharge profile obtained in a Li—N_2 cell with SnO_2 particles on nitrogen-doped carbon nanosheets (SnO_2@NC)[61] showed a reaction plateau at ≈ 1.3 V versus Li^+/Li, absent in the discharge curve of the same architecture tested in argon, suggesting that lithium nitridation reaction occurred. Ex situ analysis with XRD, time-of-flight secondary ion MS, XPS, and FTIR suggested the effective Li_3N formation and decomposition. LiOH was also detected, which could be formed both during the analysis preparation and acquisition or due to Li_3N reaction with impurities.

Yang et al. suggested the combination of two previously discussed catalysts (i.e., ruthenium and molybdenum) dispersed in sequence on nitrogen-doped carbon nanotubes by atomic layer deposition.[158] This material can modify the electronic structure and promote electronic transfer: Mo^{5+} passes to the more stable Mo^{3+} after the discharge, indicating an electron-rich state of the catalyst, able to donate electrons toward N_2 adsorption, activation, and reduction. CV of this material in a coin cell with LITFSI 1 M in TEGDME showed a reduction peak above 1.5 V versus Li^+/Li under an N_2 atmosphere. SEM, EDX, XPS, and FTIR analysis evidenced Li_3N presence, but the formation of Li_2CO_3 could not be excluded: this secondary product would limit FE in a real case NH_3 production perspective.[158]

Ruthenium nanoparticles have been tested as a catalyst also by Ma et al. in a Li—N_2 cell fed both by N_2 and saturated H_2O vapor simultaneously during discharge, to continuously produce NH_3.[27] The proposed reactions occurring in this system are:

During cell discharge:	Anode:	$6Li \rightarrow 6Li^+ + 6e^-$	(13)
	Cathode:	$6Li^+ + N_2 + 6H_2O + 6e^- \rightarrow 6LiOH + 2NH_3$	(14)
	Complete cell:	$6Li + 6H_2O_{(g)} + N_{2(g)} \rightarrow 6LiOH + 2NH_{3(g)} E^0 = 2.23 V vs Li^+/Li$	(15)
During cell charge:	Anode:	$4Li^+ + 4e^- \rightarrow 4Li$	(16)
	Cathode:	$4LiOH \rightarrow 4Li^+ + 4e^- + 2H_2O + O_2$	(17)
	Complete cell:	$4LiOH \rightarrow 4Li + 2H_2O + O_2$	(18)

Interestingly, the equilibrium potential of the proposed discharge reaction is higher than Li_3N electrochemical formation equilibrium potential: the presence of H_2O could allow the formation of new reaction intermediates and NH_3 at a cell potential less deteriorating for the electrolyte. The reported FE was 4.2% at 0.1 mA cm^{-2}, but the NH_3 yield was in a total of some μg.[27] Moreover, control tests should be assessed to exclude NH_3 spontaneously obtained from the direct reaction of the metallic lithium anode with N_2 and H_2O. NH_3 was detected only for 18 h until pore blocking due to LiOH formation and electrolyte decomposition caused complete system degradation and arrestment.

5.2.3. Beyond Li—N_2 Cells: Different Architectures and Cations

Many types of metal-gas batteries are under development and researchers are looking for new lithium-free strategies to be exploited in E-NRR studies based on metal anodes, for example, adopting sodium or aluminum.[159,160,161] An extended literature on Zn-air and Zn-N_2 batteries is under development and gaining interest as another possibility to combine energy storage and NH_3 production systems.[162,163,164] The FE values are generally limited since these systems are aqueous-based and require other tricks to reduce HER.[144]

A proof-of-concept of a Na-N_2 battery opened the applicability of cheaper and more abundant metals for mediated E-NRR stepwise approaches.[160] Ge et al. demonstrated Na_3N formation during the discharge of a cell with a sodium metal anode, $NaCF_3SO_3$ 1 M in TEGDME electrolyte, and a nano-scale wire-like α-MnO_2 catalyst on a carbon cloth cathode. The device showed good results both as the energy storage system and NH_3 production: an FE of 26% was calculated from UV-vis with NR analysis, but without carrying out isotopic labeling and NMR. The CV under N_2 presented a peculiar peak at 2 V versus Na^+/Na, associated with Na_3N formation and not relatable to intercalation, also present in argon at a lower potential.[160]

Recently, the application of a safer and more abundant metal (i.e., aluminum) has been considered and the research field on Al-air batteries is quickly growing. Al-gas devices are mainly aqueous-based,[165,166] and have also been assessed for NH_3 production.[161] An interesting result of an Al-N_2 cell for E-NRR was accomplished with an aluminum anode in an aprotic environment, with the IL AlCl/1-butyl-3-methylimidazolium chloride (1:3 w:w) as electrolyte, at a theoretical cell voltage of –1.66 V versus RHE.[161] The Gibbs' free energy of AlN is asserted as even lower than the one of Li_3N, suggesting a more spontaneous reaction, but also a more unstable product.[161] With a

graphene/Pd catalyst and a GDE architecture, the cell produced 27.1 mg g_{cat}^{-1} h^{-1} of NH_3 and an FE* of 51.2%, ten-folds the results of the same catalyst in an aqueous system.[161] After a deep discharge to 0.25 V versus RHE, the product at the cathode is soaked into NaOH 0.1 M to give the reaction:

$$AlN + NaOH + 2H_2O \rightleftarrows NaAlO_2 + NH_3 + H_2O \quad (19)$$

The CV demonstrated the presence of an electrochemical interaction at reductive potential only in the presence of N_2 (at 1.46 and 0.79 V versus Al^{3+}/Al). XRD, XPS, SEM, and high-resolution transmission electron microscopy showed AlN presence. The main drawback of the formation of AlN is its high resistivity, which limits the interaction between the cathode and fresh reactants.[161]

The possibility of exploiting different metals from lithium opens new scalable E-NRR possibilities. The production of NH_3 combined with abundant alkali salt could avoid the reduction step (from cation to element) for the adopted metal, as well as permitting a cheaper electrification of commodities obtained from NH_3, as fertilizers. However, these technologies are at the beginning of their technical assessment and materials exploration; even if they seem promising, the starting point of the well-known lithium metal systems should not be skipped for a fundamental understanding of the E-NRR process.

5.2.4. Pros and Cons of Li—N_2 Cell for Stepwise Processes and Future Outlooks for this Technology

The main advantage of this technology is the formation of nitrogen species separately from their protonation, allowing this step of the NH_3 production process to be coupled with direct H_2O protonation during the cathode washing step. In comparison with continuous electrolytic cells, this Galvanic cell is not dependent on an H_2 feed, nor on proton donor/shuttle presence in the cell, saving their production energy, as detailed in Section 6.[27] Moreover, it presents higher efficiency of lithium exploitation in comparison with direct nitridation, since only the Li^+ transported at the cathode will react with nitrogen, avoiding recycling a not negligible amount of unreactive bulky lithium particles.[136]

The Li_3N formation with a Galvanic cell, intrinsically operating at positive potentials and in which the chemical energy of a spontaneous reaction is converted into electric current, allows for recovery of the spontaneous exothermic reaction energy of this intermediate as electric energy, highly efficient and recently more and more preferred, representing an energy-saving strategy.

Moving from this technology toward different cations, such as Al^+ or Zn^+, already largely proposed in literature and discussed in Section 5.2.3, could also save the energy consumption of the reduction of the mediator and in some cases, as for K^+, could be integrated into a further process of NH_3-derived chemicals as fertilizer.[161,162]

However, some questions about this technology should still find a clear answer. First of all, the evidence of an electrochemical reaction between Li^+ and N_2, usually supported by CV with a negligible difference between tests conducted in argon or N_2 atmosphere (Section 5.2.1), is misleading, and further work is necessary toward the understanding of the reaction mechanism. The anode of lithium metal could itself spontaneously react with N_2, forming Li_3N and then NH_3, bringing to an incorrect quantification of the N_2 activated at the WE even with isotopic labeling.[25] It should be replaced with another anodic material, inert with N_2, but able to refurnish cations in the electrolyte; LIBs could be inspirational for this aim, as well as industrially interesting oxidation reactions.

Moreover, as detailed in Section 5.2.2, a catalyst might be needed to increase the N_2 activation kinetics, as well as the current density and consequently the production rate. Indeed, the NH_3 production rate is rarely evaluated for this setup but is in general inferior to continuous electrochemical strategies.[27,158] To carefully compare NH_3 yield with other strategies, the protonation step should also be detailed and deepened. The feasibility of the cathode washing directly into the cell has not yet been carefully assessed, a mobile component integrated in the process could be considered.[17]

The GDE in this architecture should present high electronic conductivity and mechanical and electrochemical stability. Moreover, to ensure a sufficient Li_3N accumulation in the porous structure, it needs a high specific surface area.[167] The pore volume should be tailored accordingly: a modulated morphology could improve the overall performance, hosting a suitable amount of the discharge product, and maintaining channels for the gas permeation, as suggested in LMBs.[146] The deposited Li_3N could slow interfacial electron transfers due to its low electronic conductivity (10^{-12} S cm^{-1}), but the high ionic conductivity (10^{-3} S cm^{-1}) is suitable for Li^+ migration.[167] Instabilities such as flooding, as well as the composition of the SEI layer, should be deepened as for electrolytic cells (Section 4.6), but in this case, the Li_3N formation is expected at a cell potential higher of ≈ 1 V in comparison with the lithium plating, meaning a lower cell potential difference and less polarization of the electrodes, leading to a moderate electrolyte species depletion.[25] For this device, it should be easier to obtain a stable SEI layer on the WE, considering also the less reactive interface in comparison with the freshly plated lithium. Studies on similar Li—O_2 batteries could be a starting point to improve the GDE stability.[168] The application of solid or gel polymer electrolyte could be a solution for a stable device, opening also to a direct protonation and washing of the cathode.[147,169]

Future insight could be obtained by studying the reaction mechanism at the WE interface with in operando techniques, as suggested in Section 2. Revealing the role of Li^+ with respect to the catalyst and N_2 is fundamental toward the understanding of the real intermediates of the reaction in this complex system.

6. Final Comparison Between Major Continuous and Discontinuous Strategies

In this review, different strategies employing lithium as a mediator for E-NRR have been described and analyzed. It is emerging how the third element in the period table presents a unique thermodynamic ability toward N_2 fixation. Moreover, the translation of NH_3 synthesis into an electrochemical process exploiting renewable energy is recognized as a profitable (to obtain an easier

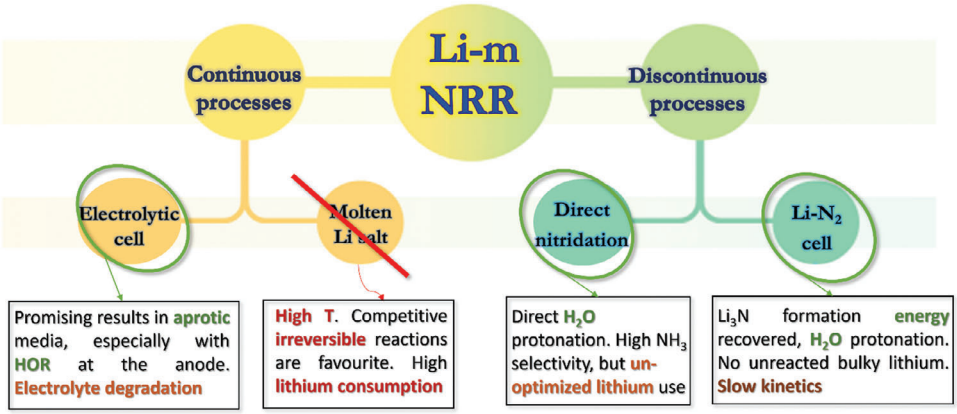

Figure 9. Classification of different Li-m E-NRR technologies with selections of the most promising systems (within the green circles) from the less emerging strategy nowadays in literature (red line). As explanation of the selection, a brief overview of main characteristics of each class is reported in the panels below.

and faster control of reaction parameters) and sustainable (with respect to the HB process) strategy in the ongoing ecological transition.

The high variability among the different systems discussed in this review does not allow a direct comparison of different operating conditions and parameters in relation to the process performance. However, the more promising and nowadays studied pathways are resumed and compared in this Section. A general outlook in this early research stage is considered useful to consciously move in this manifold panorama, to get more knowledge about the Li-m E-NRR mechanisms and avoiding to verticalize attempts in direction of only one main objective, e.g. high FEs, at the expense of other important parameters, such as production rate, stability, feasibility, and costs of reactor architectures. **Figure 9** shows the amended version of the initially shown scheme on the different Li-m E-NRR pathways, with the addition of a first distinction among less attractive and promising solutions, outlining pros and cons for each of them.

Figure 10 shows a visual qualitative comparison of the selected main Li-m E-NRR strategies. In the circular diagrams in Figure 10a, the main figures of merit (i.e., FE, NH_3 production rate, stability, scalability, and low cost) are resumed. From these charts, it is possible to observe what are the main characteristics of each technology, its strengths and limitations. Figure 10b compares different strategies within a four-variable framework: each quadrant represents one figure of merit related to yield or scalability. The center of the diagram represents the optimal process, in which each figure of merit is maximized. Low values are placed in the external corners. The strategies are set in the framework at a distance from the center qualitatively proportional to the medium of each figure of merit, better expressed for each quadrant in Figure 10c.

From the framework, it is possible to observe that the most studied electrolytic cells reached nowadays the highest NH_3 production rate and FE, also confirmed in multiple works with isotopic labeling quantification and/or with NH_3 yield far above impurities. However, this strategy still presents some technological drawbacks that have to be solved to lead to a long-term process competitive with the HB one. For this reason, the outstanding results recently obtained in the continuous aprotic Li-m E-NRR field should be considered as a starting point and not as a final outcome. The electrolyte degradation due to secondary reactions and the consequent Li^+ depletion still limit its scalability. The combination of HOR reaction and a second symbiotic H_2O-splitting cell could partially solve this problem, but it will enhance the complexity of the process and imply a higher capital cost. The SEI layer composition and stability, directly correlated to electrolyte depletion, emerged as key factors in this system (Section 4.6).[43,93,100,170]

On the other hand, the deepening of stepwise strategies opens up new interesting insights into highly selective processes. The separation of each reaction allows drawbacks for each step to be stressed, analyzed, and optimized. The understanding of mechanisms and kinetics allows the exploitation of each reactant. N_2 reduction in the absence of protons could increase Li_3N selectivity. The operation of lithium reduction in a separate step, without protons neither N_2, could avoid energy losses, e.g. in an unstable SEI layer formation. The main issue of a stepwise process could be the lower NH_3 production rate. In this panorama, Li—N_2 Galvanic cell appeared promising for an electrocatalytic N_2 fixation into Li_3N with optimized lithium amount, enhancing kinetics in comparison with the direct lithium nitridation. Moreover, the direct hydrolyzation of Li_3N into NH_3 is interesting to gain independence from unstable fossil fuel-derived proton donors or carriers. From an energetic and economic point of view, an economic analysis has been proposed for the Li-m E-NRR technology based on the three steps illustrated in Section 5.1; McEaney et al. investigated these aspects, with lithium recovery operated through the molten salt solution. They calculated a minimum electricity cost of ≈ 14 kWh kg_{NH3}^{-1} with this process, which results comparable to the HB process (≈10 kWh kg_{NH3}^{-1}), and is recalled that this new strategy presents advantages as to be easier delocalized and fed by renewables.[17] This value is an estimation for the energy cost of LiOH electrolysis at 3 V, excluding considerations of additional costs such as N_2 separation from air, NH_3 separations from the liquid aqueous output, and overpotentials in the electrochemical step. A more comprehensive and conservative calculation has been reported by Allen et al., who suggested an overall energy cost of 22 kWh kg_{NH3}^{-1} when using H_2O as a proton source.

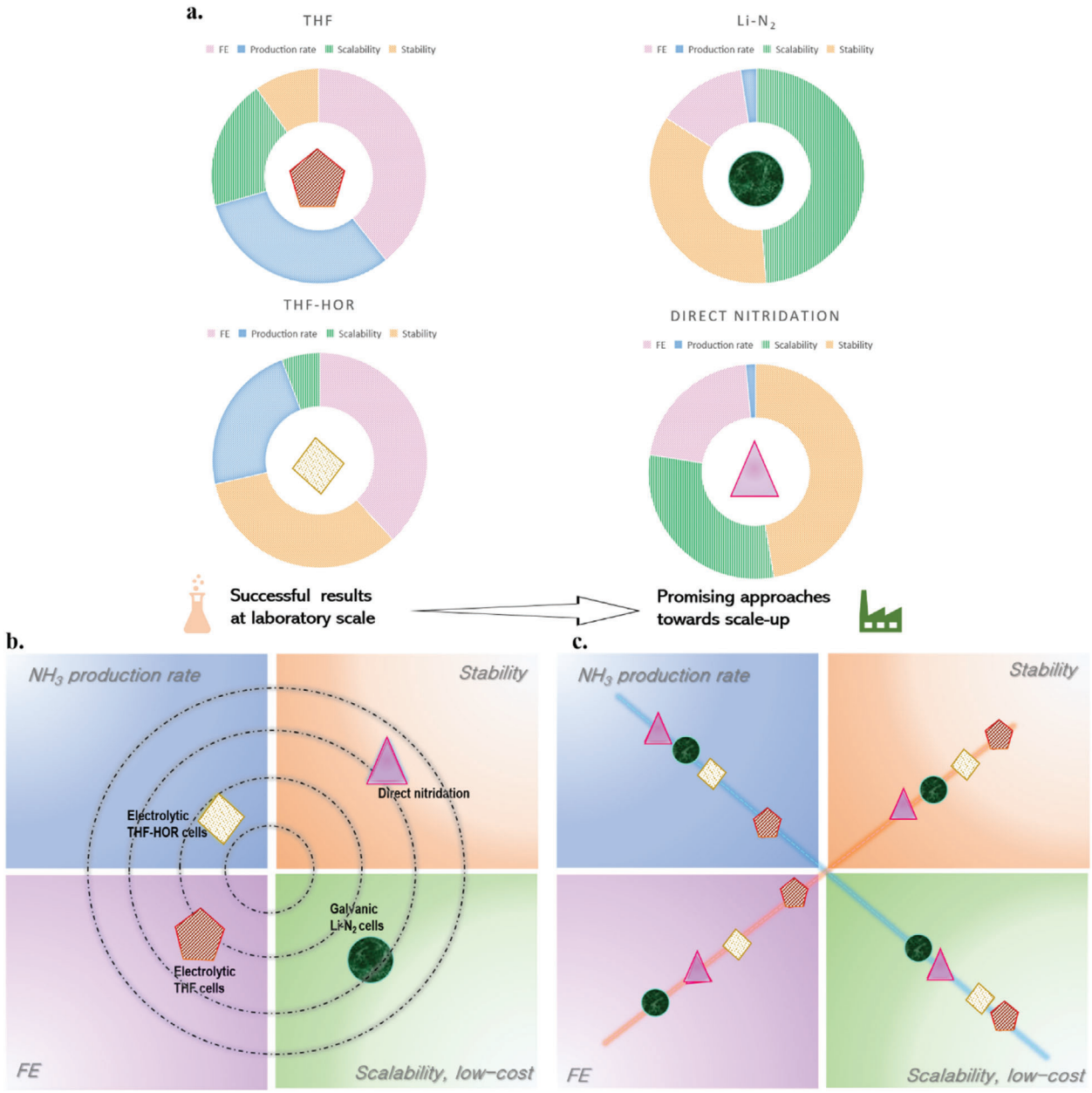

Figure 10. Qualitative resume of the main characteristics of Li-m E-NRR strategies, weighted and normalized for each approach. a) Circular diagrams for each of the main proposed methods (i.e), THF-based electrolytic cells, THF and H_2O splitting cells for HOR, working in symbiosis, Li—N_2 devices, direct nitridation strategies). b) Overall comparison of the main methods for Li-m E-NRR in a four-variables framework. The considered figures of merit are NH_3 production rate (blue), FE (violet), stability (orange), scalability, and low cost (green). The center of the diagram represents the optimal solution, the grey circles guide the comparison among the different strategies, represented by the same symbols as in panel (a) (i.e), red pentagon for electrolytic batch cell, yellow rhombus for electrolytic cell for E-NRR combined with HOR, green circle for discontinuous process with Li—N_2 cell, pink triangle for discontinuous process with direct nitridation). The strategies are set in the quadrant of each figure of merit that could best represent the main characteristic of the method) c) Comparison of the different strategies for each figure of merit: from outside to inside (with the ideal maximization of the characteristic at the middle of the figure).

This result highlighted the convenience of a direct protonation with H_2O over the combination of both electrochemical H_2 generation and E-NRR, which present a total energy demand of 26 kWh kg_{NH3}^{-1}.[171] The H_2 production would emit an average amount of more than 0.4 t_{CO2}/t_{NH3}, as proposed by Smith et al.[172] The H_2 generation cost should be considered to avoid a translation of CO_2 emissions from the steam reforming combined with direct thermochemical reaction at high pressure in HB, to H_2 electrochemical generation combined to E-NRR. Indeed, the H_2 feed is more convenient in comparison with the addition of a sacrificial organic molecule as a proton donor in the electrolyte in continuous aprotic

Li-m E-NRR electrolytic cells, but the H_2 production from fossil fuels presents nowadays higher competitiveness, and electrolyzers require precious and/or not abundant metals to reach high efficiency, even if new classes of materials are under development.[173,174]

The combination of economic study with cradle-to-gate life cycle assessment (LCA) could indicate a direction to decision-makers toward a more sustainable process. Gomez et al. assessed a preliminary economic study combined with LCA for a stepwise system, simulating mass and energy flows with the Aspen Plus process simulator.[136] Their process included N_2 separation from air by cryogenic distillation, an electrochemical reactor for lithium recovery from LiOH oxidation in H_2O and O_2, and a second electrochemical reactor for NH_3 formation, in which two reactions alternately occurred at the cathode:

$$6Li^+ + N_2 + 6e^- \rightarrow 2Li_3N \quad (20)$$

$$2Li_3N + 6H_2O \rightarrow 6LiOH + 2NH_3 \quad (21)$$

The LCA boundaries started from LiOH brine extraction, and the system was assessed for a yearly base capacity of $\approx 50 \times 10^3$ metric tons of NH_3. They supported the economic viability of this Li-m E-NRR process fed with a cheap and renewable electricity source, suggesting also an energy saving of 23% compared to systems using a proton-conducting membrane and Li-m pathway with the proton donor in the same reactor of lithium nitridation step.[136] This study concluded with an optimistic outlook: Despite the high estimated energy consumption of lithium reduction and extraction, the significant benefits of this Li-m E-NRR process were argued from different aspects. Indeed, this process could be powered without carbon emissions, adaptable to small decentralized plants, and with reduced transport costs, enabling competitivity with the HB process.[136]

In conclusion, in comparison with Li-m E-NRR continuous systems, the stepwise technology could be promising for a more durable and simplified process for NH_3 production from N_2 and H_2O. The combination of the discontinuous strategy with a Galvanic Li—N_2 cell is intriguing: this strategy presents a smaller potential window, and consequent electrode polarization, in comparison with the electrolytic cell of continuous strategy, and potentially lower energy consumption. It may increase kinetics and lithium exploitation in comparison with direct nitridation.

7. Conclusion and Future Outlook for Li-m E-NRR

A driving question in this research field should remain the following: are these newly proposed NH_3 production processes sustainable?

The NH_3-production electrification, as already stated in the Introduction, could break the wall of highly available and distributed small plants with lower capex cost and coupled with renewables, that will ensure fertilizer availability to highly populated and developing countries, bringing advantages to the 11th sustainable development goal (i.e., food availability), and ensure more independence in politics instability period. A LCA of the whole process should be conducted in parallel with technical advancements, to ensure that there will not be a mere shifting of emissions and environmental impact from HB to Li-m E-NRR. Warnings should be maintained for the environmental and safety risks of each component of the process, even more, if the management of the process is given to not highly specialized operators. H_2O-protonated systems such as Li—N_2 cells would be preferable for this purpose, as discussed in Section 6, even if the performances obtained in preliminary studies are still far from a competitive production. Future research should focus on a series of priorities, here reported.

- Face the ambiguity of very low total productions, critically revising the reproducibility and validating with a straight protocol the obtained results; if necessary, scaling the setup even in a preliminary study could be a solution to obtain reliable value.
- Sources of misunderstandings, such as NOx from N2 feed and lithium metal anode in Li—N2 cells, should be eliminated and avoided. The choice of an anodic reaction should be carefully assessed since it should be feasible and convenient at an industrial scale.
- The production rate should be considered by the scientific community at least as important as the FE, and sufficient information should be provided to correctly compare this figure of merit in different works.
- The EE assessment needs uniform boundaries for a proper comparable calculation, and should also consider the proton source, as well as lithium/Li+, production costs.
- The stability is a mandatory factor that should be discussed and addressed, in particular for the more established strategy (e.g., the SEI layer tailoring is essential for a more durable NH3 production in continuous electrolytic cells and should be deepened, also with tools such as DOE).
- For each approach, the choice of a stable reference electrode in aprotic media, such as LiFePO4, should be addressed to better understand the reaction mechanism and compare properly different electrolytes, setups, and conditions.[177]
- The understanding of the complex interfacial phenomena in these electrochemical devices should be addressed with adequate analytical techniques, e.g. with in situ and in operando analysis due to species instability.[58,96,103,175,176]

The last point is essential to address the stability challenge and requires a fair sharing of knowledge and collaboration. The general outlook provided by this review suggests the interdisciplinarity of this research field: it presents similitudes both with CO_2 reduction systems and LIBs/LMBs. Collaborations and alliances among different experts, combined with innovative analytical techniques and statistical methods such as DOE, could fasten Li-m E-NRR study toward interesting results in the near future. The production of NH_3 and other nitrogen-containing mass commodities is nowadays a growing interest, and all the difficulties described should not be enough to give up with E-NRR. For these reasons, both continuous aprotic technologies and the NH_3 production conducted in a stepwise strategy should be deepened toward a stable, scalable, and sustainable process, able to compete against the HB counterpart.

Acknowledgements

This project received funding from the European Research Council (ERC) under the European Union's Horizon 2020 research and innovation program (grant agreement No. 948769, project title: SuN_2rise). Italian Ministry of University and Research and EU Social Found are acknowledged for PON "Research and Innovation" 2014–2020 Action IV.6 initiative, granting the research contract of L.F.

Conflict of Interest

The authors declare no conflict of interest.

Keywords

electrochemical nitrogen reduction, Li nitridation, Li—N_2 cell, Lithium-mediated ammonia, Metal-N_2, SEI layer

Received: January 5, 2024
Revised: March 18, 2024
Published online: April 30, 2024

[1] J. Lim, C. A. Fern, S. W. Lee, M. C. Hatzell, C. A. Fernández, S. W. Lee, M. C. Hatzell, *ACS Energy Lett.* **2021**, *6*, 3676.
[2] D. R. MacFarlane, P. V. Cherepanov, J. Choi, B. H. R. Suryanto, R. Y. Hodgetts, J. M. Bakker, F. M. Ferrero Vallana, A. N. Simonov, *Joule* **2020**, *4*, 1186.
[3] H. Shen, C. Choi, J. Masa, X. Li, J. Qiu, Y. Jung, Z. Sun, *Chem* **2021**, *7*, 1708.
[4] G. Soloveichik, *Nat. Catal.* **2019**, *2*, 377.
[5] C. MacLaughlin, *ACS Energy Lett.* **2019**, *4*, 1432.
[6] D. R. MacFarlane, J. Choi, B. H. R. Suryanto, R. Jalili, M. Chatti, L. M. Azofra, A. N. Simonov, *Adv. Mater.* **2020**, *32*, 1.
[7] Z. J. Schiffer, K. Manthiram, *Joule* **2017**, *1*, 10.
[8] ARPA-E, *Adv. Res. Proj. Agency – Energy.* **2016**, https://arpa-e.energy.gov/.
[9] L. Hollevoet, M. De Ras, M. Roeffaers, J. Hofkens, J. A. Martens, *ACS Energy Lett.* **2020**, *5*, 1124.
[10] A. R. Singh, B. A. Rohr, M. J. Statt, J. A. Schwalbe, M. Cargnello, J. K. Nørskov, *ACS Catal.* **2019**, *9*, 8316.
[11] N. Lazouski, A. Limaye, A. Bose, M. L. Gala, K. Manthiram, D. S. Mallapragada, *ACS Energy Lett.* **2022**, *7*, 2627.
[12] L. Niu, L. An, X. Wang, Z. Sun, *J Energy Chem* **2021**, *61*, 304.
[13] J. Hou, M. Yang, J. Zhang, *Nanoscale* **2020**, *12*, 6900.
[14] Y. Sun, Y. Wang, H. Li, W. Zhang, X. M. Song, D. M. Feng, X. Sun, B. Jia, H. Mao, T. Ma, *J Energy Chem* **2021**, *62*, 51.
[15] A. Tsuneto, A. Kudo, T. Sakata, *J. Electroanal. Chem.* **1994**, *367*, 183.
[16] N. Lazouski, Z. J. Schiffer, K. Williams, K. Manthiram, *Joule* **2019**, *3*, 1127.
[17] J. M. McEnaney, A. R. Singh, J. A. Schwalbe, J. Kibsgaard, J. C. Lin, M. Cargnello, T. F. Jaramillo, J. K. Nørskov, *Energy Environ. Sci.* **2017**, *10*, 1621.
[18] Y. Liu, M. Han, Q. Xiong, S. Zhang, C. Zhao, W. Gong, G. Wang, H. Zhang, H. Zhao, *Adv. Energy Mater.* **2019**, *9*, 1.
[19] Y. Song, D. Johnson, R. Peng, D. K. Hensley, P. V. Bonnesen, L. Liang, J. Huang, F. Yang, F. Zhang, R. Qiao, A P. Baddorf, T J. Tschaplinski, N L. Engle, M. C. Hatzell, Z. Wu, D. A. Cullen, H. M. Meyer III, B. G. Sumpter, A. J. Rondinone, *Sci. Adv.* **2018**, *4*, 1.
[20] A. Guha, S. Narayanaru, N. M. Kaley, D. K Rao, J. Mondal, T. N. Narayanan, *Mater. Today Commun.* **2019**, *21*, 100700.
[21] K. Li, S. G. Shapel, D. Hochfilzer, J. B. Pedersen, K. Krempl, S. Z. Andersen, R. Sažinas, M. Saccoccio, S. Li, D. Chakraborty, J. Kibsgaard, P. C. K. Vesborg, J. K. Nørskov, I. Chorkendorff, *ACS Energy Lett.* **2022**, *7*, 36.
[22] S. Z. Andersen, M. J. Statt, V. J. Bukas, S. G. Shapel, J. B. Pedersen, K. Krempl, M. Saccoccio, D. Chakraborty, J. Kibsgaard, P. C. K. Vesborg, J. Nørskov, I. Chorkendorff, *Energy Environ. Sci.* **2020**, *13*, 4291.
[23] A. R. Singh, B. A. Rohr, J. A. Schwalbe, M. Cargnello, K. Chan, T. F. Jaramillo, I. Chorkendorff, J. K. Nørskov, *ACS Catal.* **2017**, *7*, 706.
[24] I. J. Mcpherson, T. Sudmeier, J. P. Fellowes, I. Wilkinson, T. Hughes, S. C. E. Tsang, *Angew. Chem., Int. Ed.* **2019**, *58*, 17433.
[25] Z. Zhang, S. Wu, C. Yang, L. Zheng, D. Xu, R. Zha, L. Tang, K. Cao, X. gai Wang, Z. Zhou, *Angew. Chemie – Int. Ed.* **2019**, *58*, 17782.
[26] A. Jain, H. Miyaoka, S. Kumar, T. Ichikawa, Y. Kojima, *Int J Hydrogen Energy* **2017**, *42*, 24897.
[27] X. Ma, J. Li, H. Zhou, H. Sun, *Mater. Today Energy.* **2022**, *29*, 101113.
[28] J. L. Ma, D. Bao, M. M. Shi, J. M. Yan, X. B. Zhang, *Chem* **2017**, *2*, 525.
[29] G. F. Chen, S. Ren, L. Zhang, H. Cheng, Y. Luo, K. Zhu, L. X. Ding, H. Wang, *Small Methods* **2019**, *3*, 1800337.
[30] A. Senocrate, F. Bernasconi, D. Rentsch, K. Kraft, M. Trottmann, A. Wichser, D. Bleiner, C. Battaglia, *ACS Appl. Energy Mater.* **2022**, *5*, 14504.
[31] C. H. Lee, B. Zhao, J. K. Lee, K. F. Fahy, K. Krause, A. Bazylak, *iScience* **2020**, *23*, 101094.
[32] R. Battino, T. R. Rettich, T. Tominaga, *J Phys Chem Ref Data* **1984**, *13*, 563.
[33] H. L. Du, M. Chatti, R. Y. Hodgetts, P. V. Cherepanov, C. K. Nguyen, K. Matuszek, D. R. MacFarlane, A. N. Simonov, *Nature* **2022**, *609*, 722.
[34] F. Zhou, L. M. Azofra, M. Ali, M. Kar, A. N. Simonov, C. McDonnell-Worth, C. Sun, X. Zhang, D. R. Macfarlane, *Energy Environ. Sci.* **2017**, *10*, 2516.
[35] J. Kong, H. He, *Green Energy Environ.* **2020**, *5*, 243.
[36] J. Choi, B. H. R. Suryanto, D. Wang, H. Du, R. Y. Hodgetts, F. M. F. Vallana, D. R. Macfarlane, A. N. Simonov, *Nat. Commun.* **2020**, *11*, 1.
[37] Y. Zhao, F. Wu, Y. Miao, C. Zhou, N. Xu, R. Shi, L. Z. Wu, J. Tang, T. Zhang, *Angew. Chemie – Int. Ed.* **2021**, *60*, 21728.
[38] S. Z. Andersen, V. Čolić, S. Yang, J. A. Schwalbe, A. C. Nielander, J. M. McEnaney, K. Enemark-Rasmussen, J. G. Baker, A. R. Singh, B. A. Rohr, M. J. Statt, S. J. Blair, S. Mezzavilla, J. Kibsgaard, P. C. K. Vesborg, M. Cargnello, S. F. Bent, T. F. Jaramillo, I. E. L. Stephens, J. K. Nørskov, I. Chorkendorff, *Nature* **2019**, *570*, 504.
[39] H. Liu, N. Guijarro, J. Luo, *J Energy Chem* **2021**, *61*, 149.
[40] L. Li, C. Tang, D. Yao, Y. Zheng, S. Z. Qiao, *ACS Energy Lett.* **2019**, *4*, 2111.
[41] B. Izelaar, D. Ripepi, D. D. van Noordenne, P. Jungbacker, R. Kortlever, F. M. Mulder, *ACS Energy Lett.* **2023**, *8*, 3614.
[42] J. Kibsgaard, J. K. Nørskov, I. Chorkendorff, *ACS Energy Lett.* **2019**, *4*, 2986.
[43] S. Li, Y. Zhou, K. Li, M. Saccoccio, R. Sažinas, S. Z. Andersen, J. B. Pedersen, X. Fu, V. Shadravan, D. Chakraborty, J. Kibsgaard, P. C. K. Vesborg, J. K. Nørskov, I. Chorkendorff, *Joule* **2022**, *6*, 2083.
[44] L. Zhou, C. E. Boyd, *Aquaculture* **2016**, *450*, 187.
[45] Y. Zhao, R. Shi, X. Bian, C. Zhou, Y. Zhao, S. Zhang, F. Wu, G. I. N. Waterhouse, L. Z. Wu, C. H. Tung, et al., *Adv. Sci.* **2019**, *6*, 1802109.
[46] Y. Zhao, F. Wu, Y. Miao, C. Zhou, N. Xu, R. Shi, L. Wu, J. Tang, T. Zhang, *Angew. Chem., Int. Ed.* **2021**, *60*, 21728.
[47] J. J. Giner-Sanz, G. Leverick, V. Pérez-Herranz, Y. Shao-Horn, *J. Electroanal. Chem.* **2021**, *896*, 115250.
[48] J. J. Giner-Sanz, G. M. Leverick, L. Giordano, V. Pérez-Herranz, Y. Shao-Horn, *ECS Adv* **2022**, *1*, 024501.

[49] G. Y. Duan, Y. Ren, Y. Tang, Y. Z. Sun, Y. M. Chen, P. Y. Wan, X. J. Yang, *ChemSusChem* **2020**, *13*, 88.
[50] A. C. Nielander, J. M. McEnaney, J. A. Schwalbe, J. G. Baker, S. J. Blair, L. Wang, J. G. Pelton, S. Z. Andersen, K. Enemark-Rasmussen, V. Čolić, et al., *ACS Catal.* **2019**, *9*, 5797.
[51] H. Ryu, D. Thompson, Y. Huang, B. Li, Y. Lei, *Sens Actuators Rep* **2020**, *2*, 100022.
[52] L.-F. Gao, Y. Cao, C. Wang, Xi-W Yu, W-Bo Li, Y. Zhou, B. Wang, Y.-F. Yao, C.-P. Wu, W.-J. Luo, Z.-G. Zou, *Angew. Chemie – Int. Ed.* **2021**, *60*, 5257.
[53] A. B. Moss, S. Garg, M. Mirolo, C. A. Giron Rodriguez, R. Ilvonen, I. Chorkendorff, J. Drnec, B. Seger, *Joule* **2023**, *7*, 350.
[54] R. Kas, O. Ayemoba, N. J. Firet, J. Middelkoop, W. A. Smith, A. Cuesta, *ChemPhysChem* **2019**, *20*, 2904.
[55] A. S. Malkani, M. Dunwell, B. Xu, *ACS Catal.* **2019**, *9*, 474.
[56] D. Ripepi, R. Zaffaroni, M. Kolen, J. Middelkoop, F. M. Mulder, *Sustain. Energy Fuels.* **2022**, *6*, 1945.
[57] M. Kolen, D. Ripepi, W. A. Smith, T. Burdyny, F. M. Mulder, *ACS Catal.* **2022**, 5726.
[58] K. Krempl, D. Hochfilzer, F. Cavalca, M. Saccoccio, J. Kibsgaard, P. C. K. Vesborg, I. Chorkendorff, *ChemElectroChem.* **2022**, *9*.
[59] F. C. McFarlane, E. F. Tompkins, *Trans. Faraday Soc.* **1961**, *58*, 997.
[60] A. J. Martín, T. Shinagawa, J. Pérez-Ramírez, *Chem* **2019**, *5*, 263.
[61] F. Meng, J. Qin, X. Xiong, X. Li, R. Hu, *Energy Environ. Mater.* **2022**, *66*, 1.
[62] A. Tsuneto, A. Kudo, T. Sakata, *Chem. Lett.* **1993**, *22*, 851.
[63] F. Fiehter, P. Girard, *Erlenmeyer* **1930**, *246*, 1228.
[64] T. Furukawa, Y. Hirakawa, H. Kondo, T. Kanemura, E. Wakai, *Fusion Eng. Des.* **2015**, *98–99*, 2138.
[65] T. Ludwig, A. R. Singh, J. K. Nørskov, **2020**, *124*, 26368.
[66] H. Aral, A. Vecchio-Sadus, *Encycl. Environ. Heal.* **2011**, 499.
[67] R. Sažinas, K. Li, S. Z. Andersen, M. Saccoccio, S. Li, J. B. Pedersen, J. Kibsgaard, P. C. K. Vesborg, D. Chakraborty, I. Chorkendorff, *J. Phys. Chem. Lett.* **2022**, *13*, 4605.
[68] K. Kim, C.-Y. Yoo, J.-N. Kim, H. C. Yoon, J.-I. Han, *J. Electrochem. Soc.* **2016**, *163*, F1523.
[69] X. Fu, J B. Pedersen, Y. Zhou, M. Saccoccio, S. Li, R. Sazinas, K. Li, S Z. Andersen, A. Xu, N H. Deissler, J. B. V. Mygind, C. Wei, J. Kibsgaard, P C. K. Vesborg, J K. Nørskov, Ib Chorkendorff, *Science (80-.).* **2023**, *379*, 707.
[70] X. Fu, *Mater. Today Catal.* **2023**, *3*, 100031.
[71] W. Lai, Y. Qiao, Y. Wang, H. Huang, *Adv. Mater.* **2023**, *35*, 1.
[72] K. Yang, R. Kas, W. A. Smith, T. Burdyny, *ACS Energy Lett.* **2021**, *6*, 33.
[73] N. Lazouski, M. Chung, K. Williams, M. L. Gala, K. Manthiram, *Nat. Catal.* **2020**, *3*, 463.
[74] X. Cai, Z. Shadike, X. Cai, X. Li, L. Luo, L. An, J. Yin, G. Wei, F. Yang, S. Shen, et al., *Energy Environ. Sci.* **2023**, *16*, 3063.
[75] J. H. Montoya, C. Tsai, A. Vojvodic, J. K. Nørskov, *ChemSusChem* **2015**, *8*, 2180.
[76] X. Z. Jr, S. Mou, Q. Peng, Q. Liu, Y. Luo, G. Chen, S. Gao, X. Sun, *J Mater Chem A Mater* **2020**, *8*, 1545.
[77] G. Energy, M. Ibrar, D. Brynn, C. Zhao, *Green Energy Environ.* **2022**, 1567.
[78] Y. C. Hao, Y. Guo, L. W. Chen, M. Shu, X. Y. Wang, T. A. Bu, W. Y. Gao, N. Zhang, X. Su, X. Feng, et al., *Nat. Catal.* **2019**, *2*, 448.
[79] J. Choi, H. L. Du, M. Chatti, et al., *Nat. Catal.* **2022**, *5*, 82.
[80] Y. C. Hao, L. W. Chen, A. X. Yin, *Nat. Catal.* **2022**, *5*, 385.
[81] A. Bagger, H. Wan, I. E. L. Stephens, J. Rossmeisl, *ACS Catal.* **2021**, *11*, 6596.
[82] L. Suo, O. Borodin, T. Gao, M. Olguin, J. Ho, X. Fan, C. Luo, C. Wang, K. Xu, *Science (80-.).* **2015**, *350*, 938.
[83] J. Zhao, B. Wang, Q. Zhou, H. Wang, X. Li, H. Chen, Q. Wei, D. Wu, Y. Luo, J. You, et al., *Chem. Commun.* **2019**, *55*, 4997.
[84] G. F. Chen, X. Cao, S. Wu, X. Zeng, L. X. Ding, M. Zhu, H. Wang, *J. Am. Chem. Soc.* **2017**, *139*, 9771.
[85] D. Johnson, A. Djire, *Adv. Mater. Interfaces.* **2023**, *2202147*, 1.
[86] B. Qin, Y. Li, Q. Zhang, G. Yang, H. Liang, F. Peng, *Nano Energy* **2020**, *68*, 1.
[87] W. Gu, Y. Guo, Q. Li, Y. Tian, K. Chu, *ACS Appl Mater Interfaces* **2020**, *12*, 37258.
[88] C. Li, J. Yu, L. Yang, J. Zhao, W. Kong, T. Wang, A. M. Asiri, Q. Li, X. Sun, *Inorg Chem* **2019**, *58*, 9597.
[89] B. Flamme, G. Rodriguez Garcia, M. Weil, M. Haddad, P. Phansavath, V. Ratovelomanana-Vidal, A. Chagnes, *Green Chem.* **2017**, *19*, 1828.
[90] J. Humphreys, R. Lan, S. Tao, *Adv. Energy Sustain. Res.* **2021**, *2*, 2000043.
[91] X. Cai, C. Fu, H. Iriawan, F. Yang, A. Wu, L. Luo, S. Shen, G. Wei, Y. Shao-Horn, J. Zhang, *iScience* **2021**, *24*, 103105.
[92] J. A. Schwalbe, M. J. Statt, C. Chosy, A. R. Singh, B. A. Rohr, A. C. Nielander, S. Z. Andersen, J. M. McEnaney, J. G. Baker, T. F. Jaramillo, et al., *ChemElectroChem* **2020**, *7*, 1513.
[93] H. L. Du, K. Matuszek, R. Y. Hodgetts, K. N. Dinh, P. V. Cherepanov, J. M. Bakker, D. R. Macfarlane, A. N. Simonov, *Energy Environ. Sci.* **2023**, *16*, 1082.
[94] K. Krempl, J. B. Pedersen, J. Kibsgaard, P. C. K. Vesborg, I. Chorkendorff, *Electrochem. Commun.* **2022**, *134*, 107186.
[95] E. Peled, S. Menkin, *J. Electrochem. Soc.* **2017**, *164*, A1703.
[96] E. J. McShane, M. Cargnello, *Nat. Energy.* **2023**, *8*, 115.
[97] M. Alidoost, A. Mangini, F. Caldera, A. Anceschi, J. Amici, *Chemistry* **2022**, *28*, 1.
[98] O. Westhead, M. Spry, A. Bagger, Z. Shen, H. Yadegari, S. Favero, R. Tort, M.-M. Titirici, M. P. Ryan, R. Jervis, et al., *J Mater Chem* **2022**, *11*, 12746.
[99] J. Bjarke Valbæk Mygind, J B. Pedersen, K. Li, N H. Deissler, M. Saccoccio, X. Fu, S. Li, R. Sazinas, S Z. Andersen, K. Enemark-Rasmussen, P C. K. Vesborg, J. Doganli-Kibsgaard, Ib Chorkendorff, *ChemSusChem.* **2023**, *16*, 02301011.
[100] N. Lazouski, K. J. Steinberg, M. L. Gala, D. Krishnamurthy, V. Viswanathan, K. Manthiram, *ACS Catal.* **2022**, *12*, 5197.
[101] S. J. Blair, M. Doucet, J. F. Browning, K. Stone, H. Wang, C. Halbert, J. Avilés Acosta, J. A. Zamora Zeledón, A. C. Nielander, A. Gallo, et al., *ACS Energy Lett.* **2022**, 1939.
[102] B. H. R. Suryanto, K. Matuszek, J. Choi, R. Y. Hodgetts, H. L. Du, J. M. Bakker, C. S. M. Kang, P. V. Cherepanov, A. N. Simonov, D. R. MacFarlane, *Science (80-.).* **2021**, *372*, 1187.
[103] K. Steinberg, X. Yuan, N. Lazouski, C. K. Klein, K. Manthiram, Y. Li, *Nat. Energy.* **2023**, *8*, 138.
[104] D. Krishnamurthy, N. Lazouski, M. L. Gala, K. Manthiram, V. Viswanathan, *ACS Cent. Sci.* **2021**, *7*, 2073.
[105] R. Y. Hodgetts, H. L. Du, T. D. Nguyen, D. Macfarlane, A. N. Simonov, *ACS Catal.* **2022**, *12*, 5231.
[106] T. Li, X. Zhang, P. Shi, Q. Zhang, *Joule* **2019**, *3*, 2647.
[107] S. Kim, S. O. Park, M. Y. Lee, J. A. Lee, I. Kristanto, T. K. Lee, D. Hwang, J. Kim, T. U. Wi, H. W. Lee, et al., *Energy Storage Mater.* **2022**, *45*, 1.
[108] P. V. Cherepanov, M. Krebsz, R. Y. Hodgetts, A. N. Simonov, D. R. Macfarlane, *J Phys Chem* **2021**, *125*, 11402.
[109] R. Sažinas, S. Z. Andersen, K. Li, M. Saccoccio, K. Krempl, J. B. Pedersen, J. Kibsgaard, P. C. K. Vesborg, D. Chakraborty, I. Chorkendorff, *RSC Adv.* **2021**, *11*, 31487.
[110] W. Dekant, *Regul Toxicol Pharmacol* **2019**, *109*, 104499.
[111] M. Spry, O. Westhead, R. Tort, B. Moss, Y. Katayama, M. Titirici, I. E. L. Stephens, A. Bagger, *ACS Energy Lett.* **2023**, *8*, 1230.
[112] K. Li, S Z. Andersen, M J. Statt, M. Saccoccio, V J. Bukas, K. Krempl, R. Sazinas, J. B. Pedersen, V. Shadravan, Y. Zhou, D. Chakraborty, J.

Kibsgaard, P C. K. Vesborg, J K. Nørskov, Ib Chorkendorff, *Science (80-.)*. **2021**, *374*, 1593.
[113] E. J. Mcshane, P. Benedek, V. A. Niemann, S. J. Blair, G. A. Kamat, A. C. Nielander, T. F. Jaramillo, M. Cargnello, *ACS Energy Lett.* **2023**, *8*, 230.
[114] R. Tort, O. Westhead, M. Spry, B. J. V. Davies, M. P. Ryan, M. M. Titirici, I. E. L. Stephens, *ACS Energy Lett.* **2023**, *8*, 1003.
[115] R. Leardi, *Anal Chim Acta* **2009**, *652*, 161.
[116] T. Murakami, T. Nishikiori, T. Nohira, Y. Ito, *J. Am. Chem. Soc.* **2003**, *125*, 334.
[117] N. Serizawa, H. Miyashiro, K. Takei, T. Ikezumi, T. Nishikiori, Y. Ito, *J. Electrochem. Soc.* **2012**, *159*, E87.
[118] M. Ravi, J. W. Makepeace, *Chem. Commun.* **2022**, *58*, 6076.
[119] K. Tagawa, H. Gi, K. Shinzato, H. Miyaoka, T. Ichikawa, *J Phys Chem* **2022**, *126*, 2403.
[120] P. Wang, F. Chang, W. Gao, J. Guo, G. Wu, T. He, P. Chen, *Nat. Chem.* **2017**, *9*, 64.
[121] M. Yang, U. Raucci, M. Parrinello, *Nat. Catal.* **2023**, *6*, 829.
[122] K. Shinzato, K. Tagawa, K. Tsunematsu, H. Gi, P. K. Singh, T. Ichikawa, H. Miyaoka, *ACS Appl. Energy Mater.* **2022**, *5*, 4765.
[123] A. Jain, H. Miyaoka, T. Ichikawa, *Int J Hydrogen Energy* **2016**, *41*, 5969.
[124] Y. Kojima, H. Miyaoka, Y. Shotaro, I. Takayuki, W. Yongming, N. Yui, I. Shigehito, K. Yoshitsugu, M. Hiroki, *ACS Omega* **2017**, *2*, 1081.
[125] T. Yamaguchi, K. Shinzato, K. Yamamoto, *Int J Hydrogen Energy* **2020**, *45*, 6806.
[126] Z. Tang, X. Meng, Y. Shi, X. Guan, *ChemSusChem* **2021**, *14*, 4697.
[127] S. Licht, B. Cui, B. Wang, F. F. Li, J. Lau, S. Liu, *Science (80-.)*. **2014**, *345*, 637.
[128] S. Licht, B. Cui, B. Wang, F.-F. Li, J. Lau, S. Liu, *Science (80-.)*. **2020**, *369*, 780.
[129] and C. G. Bonomi, A. M. Hadate, *J. Electrochem. Soc.* **1977**, *124*, 78.
[130] G. Miceli, C. S. Cucinotta, M. Bernasconi, M. Parrinello, *J Phys Chem* **2010**, *114*, 2645.
[131] J. W. Makepeace, T. J. Wood, H. M. A. Hunter, M. O. Jones, W. I. F. David, *Chem. Sci.* **2015**, *6*, 3805.
[132] R. Michalsky, A. M. Avram, B. A. Peterson, P. H. Pfromm, A. A. Peterson, *Chem. Sci.* **2015**, *6*, 3965.
[133] D. V Shchur, S. Y. Zaginaichenko, A. Veziroglu, T. N. Veziroglu, N. A. Gvrylyuk, A. D. Zolotarenko, M. T. Gabdullin, *Russ. Phys. J.* **2021**, *64*, 89.
[134] J. W. Makepeace, J. M. Brittain, S. Manghnani, C. A. Murray, J. Wood, W. I. F. David, *Phys. Chem. Chem. Phys.* **2021**, *23*, 15091.
[135] Q. R. Wang, Y. Q. Guan, W. B. Gao, J. P. Guo, P. Chen, *ChemPhysChem* **2019**, *20*, 1376.
[136] J. R. Gomez, *Int. J. Energ. Res.* **2021**, *46*, 13461.
[137] Z. Zhang, Y. Zhao, B. Sun, J. Xu, Q. Jin, H. Lu, N. Lyu, Z. M. Dang, Y. Jin, *ACS Appl Mater Interfaces* **2022**, *14*, 19419.
[138] K. Kim, J. Lee, D. Kim, C. Yoo, W. Choi, *ChemSusChem* **2018**, *11*, 120.
[139] K. Kim, J. E. Soc, K. Kim, H. Cho, S. H. Jeon, S. J. Lee, C. Yoo, J. Kim, J. W. Choi, H. C. Yoon, et al., *J. Electrochem. Soc.* **2018**, *165*, F1027.
[140] K. Kim, Y. H. Chen, C. Jong-In, H. Yoonc, L. Wenzhen, *Green Chem.* **2019**, *21*, 3839.
[141] I. A. Amar, R. Lan, C. T. G. Petit, S. Tao, *J. Solid State Electrochem.* **2011**, *15*, 1845.
[142] Y. Ding, J. Zhang, A. Guan, Q. Wang, S. Li, A. M. Al Enizi, L. Qian, *Nano Converg* **2021**, *8*, 14.
[143] F. Wang, X. Li, X. Hao, J. Tan, *ACS Appl. Energy Mater.* **2020**, *3*, 2258.
[144] J. Islam, M. Shareef, H. M. Zabed, X. Qi, F. I. Chowdhury, J. Das, J. Uddin, Y. V. Kaneti, M. U. Khandaker, M. H. Ullah, et al., *Energy Storage Mater.* **2023**, *54*, 98.
[145] X. G. Wang, Q. Zhang, X. Zhang, C. Wang, Z. Xie, Z. Zhou, *Small Methods* **2019**, *3*, 1.
[146] R. Black, B. Adams, L. F. Nazar, *Adv. Energy Mater.* **2012**, *2*, 801.
[147] J. Amici, G. Banaudi, M. Longo, M. Gandolfo, M. Zanon, C. Francia, S. Bodoardo, M. Sangermano, *Polymers (Basel)* **2023**, *15*, 3182.
[148] I. Matanovic, F. H. Garzon, *Phys. Chem. Chem. Phys.* **2018**, *20*, 14679.
[149] Z. Zhang, J. Bao, C. He, Y. Chen, J. Wei, Z. Zhou, *Adv. Funct. Mater.* **2014**, *24*, 6826.
[150] H. Dong, W. Xu, J. Xie, Y. min Ding, Q. Wang, L. Zhou, *Appl. Surf. Sci.* **2022**, *604*, 154507.
[151] H. Zhong, M. Wang, M. Ghorbani-Asl, J. Zhang, K. H. Ly, Z. Liao, G. Chen, Y. Wei, B. P. Biswal, E. Zschech, et al., *J. Am. Chem. Soc.* **2021**, *143*, 19992.
[152] F. Liu, L. Song, Y. Liu, F. Zheng, L. Wang, K. Palotás, H. Lin, Y. Li, *J Mater Chem* **2020**, *8*, 3598.
[153] Y. Wang, W. Cheng, P. Yuan, G. Yang, S. Mu, J. Liang, H. Xia, K. Guo, M. Liu, S. Zhao, et al., *Adv. Sci.* **2021**, *8*, 1.
[154] S. Yi, G. Liu, Z. Liu, W. Hu, H. Deng, *J Mater Chem* **2019**, *7*, 19950.
[155] J. Amici, P. Marquez, A. Mangini, C. Torchio, D. Dessantis, D. Versaci, C. Francia, M. J. Aguirre, S. Bodoardo, *J Power Sources* **2022**, *546*, 231942.
[156] D. Versaci, A. Costanzo, S. M. Ronchetti, B. Onida, J. Amici, C. Francia, S. Bodoardo, *Electrochim. Acta*. **2021**, *367*, 137489.
[157] L. L. Zhang, M. Cong, X. Ding, Y. Jin, F. Xu, Y. Wang, L. Chen, L. L. Zhang, *Angew. Chem., Int. Ed.* **2020**, *59*, 10888.
[158] Y. Yang, N. Zhang, Z. Zou, X. Yi, J. Liu, *Chem. Eng. J.* **2022**, *435*, 135148.
[159] F. Meng, X. Xiong, S. He, Y. Liu, R. Hu, *Adv. Energy Mater.* **2023**, *2300269*, 1.
[160] B. Ge, Y. Wang, Y. Sun, Y. Li, J. Huang, Q. Peng, *Energy Storage Mater.* **2019**, *23*, 733.
[161] Y. Guo, Q. Yang, D. Wang, H. Li, Z. Huang, X. Li, Y. Zhao, B. Dong, C. Zhi, *Energy Environ. Sci.* **2020**, *13*, 2888.
[162] G. Nam, H. Jang, J. Sung, S. Chae, L. Soule, B. Zhao, J. Cho, M. Liu, *ACS Appl Mater Interfaces* **2020**, *12*, 57064.
[163] H. Wang, Z. Li, Y. Li, B. Yang, J. Chen, L. Lei, S. Wang, Y. Hou, *Nano Energy* **2021**, *81*, 05613.
[164] H. Qiao, Y. Han, L. Yao, X. Xu, J. Ma, B. Wen, J. Hu, H. Huang, *Chem. Eng. J.* **2023**, *464*, 142628.
[165] T. Wang, Z. Tian, Z. You, Z. Li, H. Cheng, W. Li, Y. Yang, Y. Zhou, Q. Zhong, Y. Lai, *Energy Storage Mater.* **2022**, *45*, 24.
[166] R. Buckingham, T. Asset, P. Atanassov, *J Power Sources* **2021**, *498*, 229762.
[167] J. H. Kang, J. Lee, J. W. Jung, J. Park, T. Jang, H. S. Kim, J. S. Nam, H. Lim, K. R. Yoon, W. H. Ryu, et al., *ACS Nano* **2020**, *14*, 14549.
[168] Y. Zhou, S. Guo, *eScience* **2023**, *3*, 100123.
[169] Q. Zhu, J. Ma, S. Li, D. Mao, *Polymers (Basel)* **2023**, *15*, 2469.
[170] K. Steinberg, X. Yuan, C. Klein, N. Lazouski, M. Mecklenburg, K. Manthiram, Y. Li, *ECS Meet. Abstr.* **2022**, *MA2022-02*, 2526.
[171] J. Allen, S. Panquet, A. Bastiani, *Front Chem Eng* **2021**, *3*, 1.
[172] C. Smith, A. K. Hill, L. Torrente-Murciano, *Energy Environ. Sci.* **2020**, *13*, 331.
[173] M. Chatenet, B. G. Pollet, D. R. Dekel, F. Dionigi, J. Deseure, P. Millet, R. D. Braatz, M. Z. Bazant, M. Eikerling, I. Staffell, et al., *Chem. Soc. Rev.* **2022**, *51*, 4583.
[174] Z. W. She, J. Kibsgaard, C. F. Dickens, I. Chorkendorff, J. K. Nørskov, T. F. Jaramillo, *Science (80-.)*. **2017**, *355*, aad4998.
[175] H. Li, W. Wang, *Curr. Opin. Electrochem.* **2023**, *41*, 101376.
[176] X. Zhang, Y. Lyu, H. Zhou, J. Zheng, A. Huang, J. Ding, C. Xie, R. De Marco, N. Tsud, V. Kalinovych, S. P. Jiang, L. Dai, S. Wang, *Adv. Mater.* **2023**, *35*, 1.
[177] F. La Mantia, C. D. Wessells, H. D. Deshazer, Y. Cui, *Electrochem. Commun.* **2013**, *31*, 141.

Anna Mangini is a PhD student in Materials Science and Technology in the Electrochemistry Group at Politecnico di Torino (Italy), under the supervision of Prof. Bella. She received a BSc degree in Materials Engineering in 2018 and an MSc degree in Chemical Engineering in 2020 from the same institution. She formerly carried out a research fellowship on lithium-metal batteries for both high-power and energy-density sustainable applications. She has also worked on silicon-enriched anodes for lithium-ion batteries. Her current activity is focused on N_2 reduction reactions based on lithium-mediated pathways.

Lucia Fagiolari is Assistant Professor at Politecnico di Torino (Italy). She works in the Electrochemistry Group. Formerly involved in the "SuN_2rise" ERC-StG project led by Prof. Bella, she is now active on a 3-year project funded by both the Italian Ministry of University and Research and Casale SA company, dealing with the sustainable production of ammonia. Her research is currently focused on Li/N_2 cells for the electrochemical production of ammonia and fertilizers. She is the author of 21 publications (*h*-index 17) and is a Permanent Editor in Frontiers in Chemistry.

Annalisa Sacchetti is the Laboratory Section Manager in Casale SA (Lugano, Switzerland). She received her PhD in Industrial Chemistry at the University of Bologna, working on the synthesis and testing of catalysts for bio-oil valorization. Since 2021, she has been working in the R&D Division of Casale SA and she is now following the experimental activities carried out in the R&D Casale Laboratory.

Alberto Garbujo is a Senior Research Engineer in Casale SA (Lugano, Switzerland). He received his PhD from the University of Padua (Italy), working on high-temperature fuel cells. Since 2018, he has been working in the R&D Division of Casale SA, where he supervises catalysis and electrocatalysis research activities. His work mainly focuses on ammonia and nitrate production, as well as environmental catalysis. He is the author of 16 publications and 5 patent applications. He has been a guest editor for Catalysis Today for the special issue entitled "100 Years of Casale SA".

Pierdomenico Biasi is the Department Head of Basic Research in Casale SA (Lugano, Switzerland). He works in the R&D Division leading the activities in catalysis, biotechnologies, and future technologies. He received the Sandmeyer Award for the development and implementation of the AmoMax-Casale catalyst from the Swiss Chemical Society. He is the author of 40 publications and 10 patents, and he is on the Advisory Board of the National Centre of Competence in Research in Switzerland and in the Catalysis Today journal. He is Lecturer at École Polytechnique Fédérale de Lausanne, ETH Zürich, University of Padova, and University of Valladolid.

Federico Bella is a Full Professor of Fundamentals of Chemical Technologies at Politecnico di Torino (Italy). He works in the Electrochemistry Group, leading the research activities on solar fuels and post-lithium batteries. He has recently received the "Tajima Prize" from the International Society of Electrochemistry. He is the author of 110 publications (h-index 72) and is a member of the Editorial Board of *ChemSusChem* and *Energy Storage Materials*. He is the Vice-President of the Italian Chemical Society and leads the ERC-StG "SuN$_2$rise" project on sun-powered electrochemical nitrogen reduction.